Department of Precision and Microsystems Engineering

Design of compliant valves that can be integrated into a fluidic network

K.M.Guurink

Report no : 2023.003
Supervisor : Dr.ir A. Hunt
Specialisation : Mechatronic System Design
Type of report : Master of Science Thesis
Date : 09-01-2023

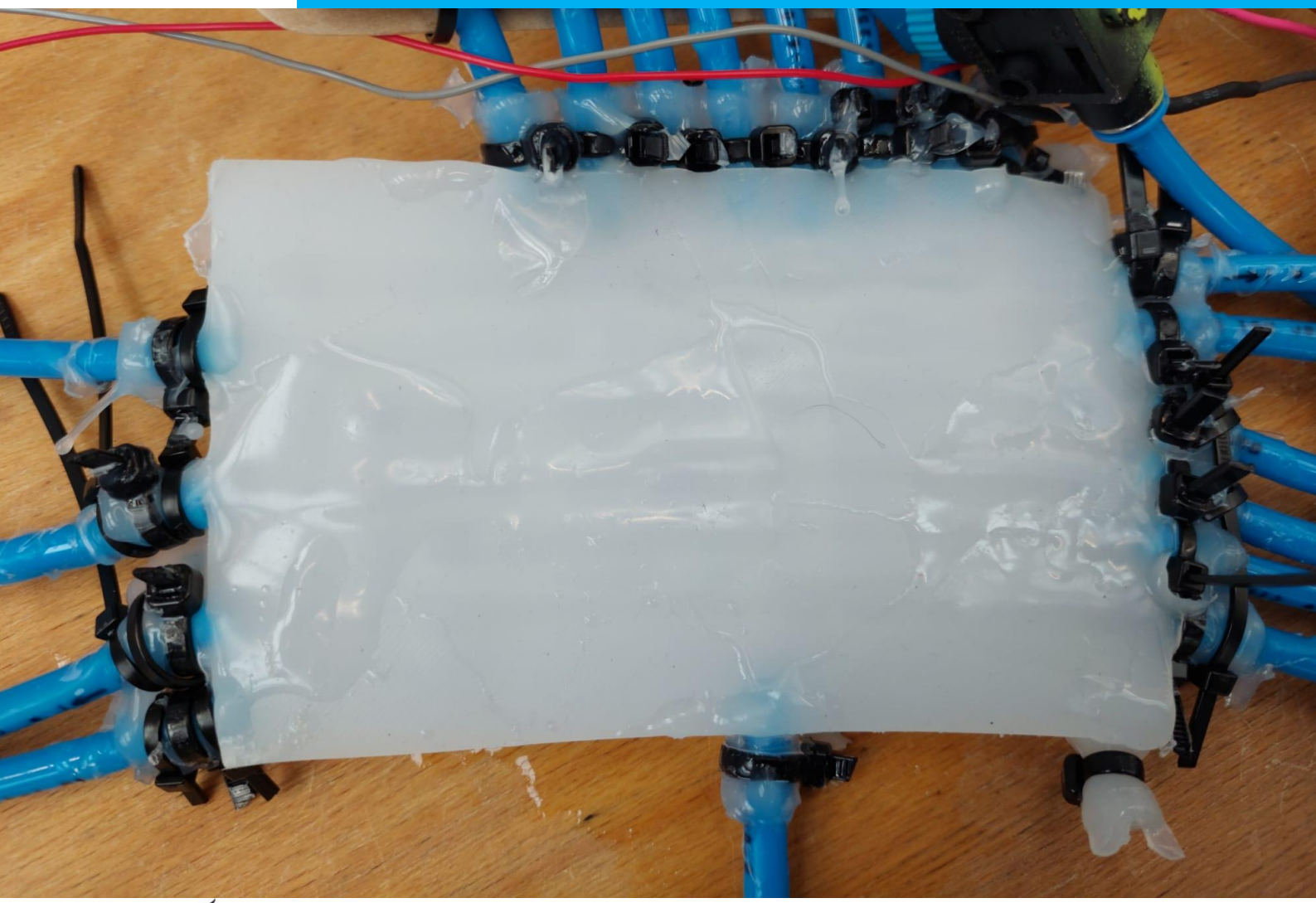

TU Delft Delft University of Technology

Challenge the future

1 Abstract

Building a distributed fluidic actuation system is a challenge due to every actuator needs its own control valve. Due to this, an n by an array of actuators needs n^2 number of valves. A logic network of valves provides a solution by reducing the number of valves needed to operate such distributed fluidic actuation system. These compliant fluidic networks could have a broad application in different fields such as biomedical, microfluidics, or in soft robotics. An example in the biomedical field is for creating an actuated surface that is controlled by a fluidic logic that goes around a hollow organ. This sleeve could provide support to the organ by externally providing actuation.

The main goal of the paper is to design a compliant valve that easily could be integrated into a large fluidic logic network, to demonstrate the network a demultiplexer is built. Compliant is defined as soft material (small E modules) with hyperplastic properties. To get a better understanding of what is already done in the field of distributed actuation systems a literature study is conducted. The thesis will provide information on the design steps of creating a valve and how to integrate them in a fluidic network that is a demultiplexer.

The operating principle of this valve is that there are 2 channels on top of each other on a 90-degree angle, one channel will be inflated and will choke the other channel. Different valve designs based on this principle have been built and tested using different shapes and combinations of materials. Using FEM software the closing pressure is calculated. After that prototypes have been built and experiments are conducted. During experiments, the pressure drop has been measured in the channel that will be closed. The next step is to understand how these valves operate in a large network. A Simulink model of a demultiplexer has been built, it was shown that 2.4 seconds to inflate an array of 8 small bellow actuators with a stroke of 5 mm. After simulating a demultiplexer is created. Experimental results show that the best-performing valve completely closes a line with a pressure of 12 kPa with an operating pressure of 26 kPa. As a demonstrator of a large-scale network a demultiplexer is built, unfortunately, it did not perform due to manufacturing problems.

To answer the main question of this paper a fully functioning logic network has not yet been achieved however, it could be said that this paper has laid a good foundation for further improvement of the creation of a scalable solution for an actuating surface. It also has to be noted that the valve designs that are discussed in this paper operate on an mm scale instead of an cm-scale which is commonly found in the literature.

Keywords: Soft robotics, compliant valves, fluidic logic gates.

2 Acknowledgements

During the thesis many people helped and supported me, and in this section I liked to thank them. Firstly I like to thank Andres Hunt for guiding me during this project. His feedback and good discussion really helped my progress, without it this thesis would not be possible. I want to thank my girlfriend Piebeth for her support during this time. Great thanks go to my parents Gerard and Conny and my brother Frank. Special thanks to my dad for the technical advice and editing during my thesis. Great thanks goes to the PME lab support for providing assistance with the experimentation. I also want to thank Oskar and Anil for providing me with the opportunity to see an operating room in action.

Koen Guurink

Rijswijk, January 2023

Contents

3 Introduction

A compliant actuated surface is a 2D array of compliant actuators that can be reconfigured. Compliant is defined as soft material (small E modules) with hyperelastic properties. On such a surface, each actuator has its own valve. Meaning for a 5 by 5 array of actuators there need to be 25 valves to control it. This means for an n by n array of actuators n^2 of valves are needed, the required valves scale exponentially. The use of rigid valves also reduces the application area because rigid valves need to control these actuator arrays externally. Soft valves can be used in to integrate these in a completely soft fluidic network that could reduce the required valves.

Networks that are made of fully compliant valves could also provide benefits in different fields for example in biomedical, microfluidics, and soft robotics. An example in the biomedical field is for creating a sleeve around a hollow organ. This sleeve could provide support to the organ by externally providing actuation. This action helps to reach the organ to the required movement to operate properly. An example in the field of microfluidics is a lab on a chip. This chip could be made from fully compliant material and then implemented in an environment were compliant matching is an important criterion, for example, where there is contact between an organ and a chip. Applications in the field of soft robotics are that soft robots could execute more complex tasks due to having access to a bigger network of logic gates.

The first step is to look at the state of the art, a literature survey is done on soft valves and compliant surfaces and logic circuits. The complete literature study can be found in Appendix A, in the section below a short version is shown. Different compliant surfaces have been researched [3] [8] [2] [5] [7]. These surfaces were all controlled in a way that each actuator's had its own valve. Other works [10] [6] also controlled an array of actuators, but used a network of microfluidic valves that functions as a demultiplexer, this reduced the required inputs to control such array. All these works controlled their actuators with rigid valves. To create a network that is fully compliant soft valves are required. Fully compliant valves have been explored [4] [9]. These valves had roughly the dimension of 3x3x4 cm. During this literature survey, the knowledge gap has been identified that there are no large fluidic networks of valves that are fully compliant. This is needed to improve the scalability, control ability, and cost of a soft-actuated surface. This thesis will consider the design and experimenting of a fully compliant valve that is integrable into a large fluidic logic network that is a demultiplexer.

This theisis consist of: Design, analysis, experimental setup, and manufacturing of complaint valves and the demultiplexer.

Design found in subsection 4.1 goes in-depth about the chosen design of the valves and of the demultiplexer. The analysis found in subsection 4.2 provided information how FEM simulations of the valves and simulations of a fluidic network with complaint valves were done. Information about experimental setup can be found in subsection 4.3, which describes how experiments were conducted for the valves and logic networks discussed under subsection design. Manufacturing found in subsection 4.4 provides information about constructing the valves and networks. In section 5 is where the experimental en analytical results are presented of the valves and demultiplexer and are discussed in section 6. The thesis ends with a conclusion and recommendation found in section 7 and section 8. All the digital files that are used during this thesis can be found in Appendix B.

4 Methodology

In this section the design strategy for the valves are discussed in subsection 4.1. FEM analysis is discussed in subsection 4.2. Information about the experimental setup can be found in subsection 4.3. The method of manufacturing can be found in subsection 4.4.

4.1 Design valves and logic circuits

In this section, information is given about the different designs. In subsubsection 4.1.1 more information is given about the valve normally open valve design. Information of the normally closed valve design is found in subsubsection 4.1.2. In subsubsection 4.1.3 information is given on how these valves can be implemented in a larger logic scheme that has fewer inputs than outputs.

4.1.1 Compliant normally open valve

The compliant normally open valve is based on a quake valve used in microfluidics. A microfluidic quake valve consists of 2 layers of rigid materials with channels in the materials and a compliant material commonly PDMS (Polydimethylsiloxaan) sandwiched in between. The working principle is that the control line (the line inflated) pushes a flexible membrane into the supply line (the one getting closed), as seen in Figure 1. This operating principle was chosen because it was proven to work in a rigid microfluidic setting.

The major difference between a microfluidics quake valve and a compliant valve is the scale, the valve in this paper is in the millimeter range instead of the micrometer range. The surrounding material is also compliant instead of rigid, this has an effect on the working principle of the valve. One of the most rudimentary compliant valves can be seen in Figure 2a.

The dimension of the control line is 1x5 mm, and the supply line is an oval shape with 1.06x6 mm in dimensions. The membrane has a thickness of 1 mm. The combination of shapes was selected after a preliminary FEM study for the best closing combination.

The Boolean logic that this type of valve design enables is that of an inverter with an AND gate where its input is connected to the output of the inverter.

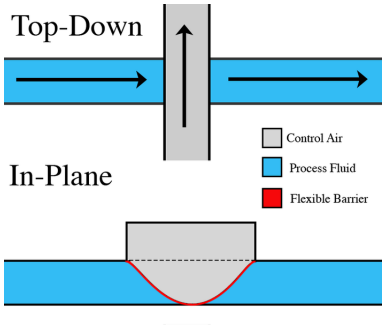

Figure 1: Working principle quake valve in micro fluidics

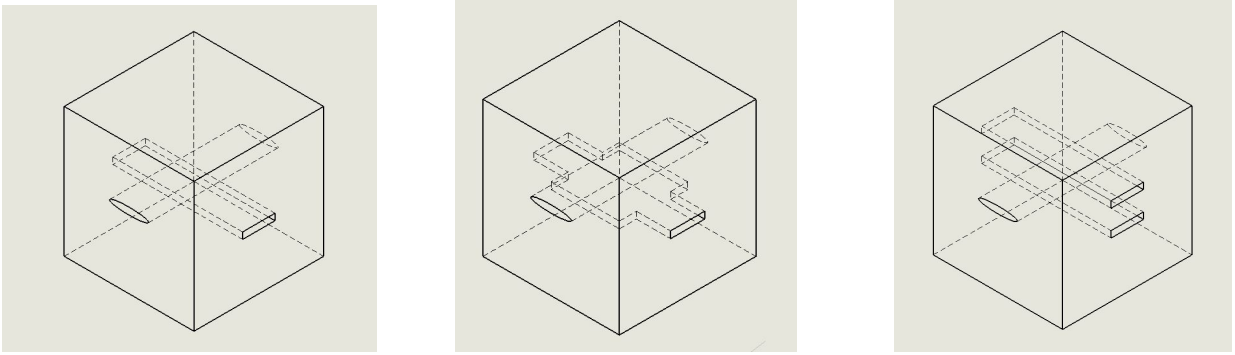

(a) quake valve (b) 10 x 10 mm valve (c) double valve

Figure 2: section different valves

The performance of the valve defined in this thesis is the pressure required to completely close the supply line, meaning which pressure of the control line results in a 0 pressure in the supply line. When rigid valves are mentioned in this paper it means a more conventional type of valve, in other words, something that can be bought off the shelf.

In the section below multiple designs are explained and the reasons why they were explored.

To increase the performance multi-material layered valves have been explored, different material properties could change the performance of the valve. A more ridged top and bottom would reduce the unwanted

deformation of the lines. A more compliant membrane would close the supply line easier, due to requiring less pressure to deform.

To increase performance a design is considered using rigid materials to constrain deformation in the out-of-plane direction. The reason for this was that this would stop undesired upwards deformations of the control line and thus increase performance. Reinforcing is achieved by using: plates, rope reinforced, cage and tiewraps. More information about the implementation can be found in subsection 4.3

Another way to improve the performance is to increase the surface area of the control line, this would increase the area and thus increase the force with the same pressure. A schematic can be found in Figure 2b. The dimension 10x10 mm has been chosen for being 2 times as large as the valve seen in Figure 2a while also remaining relatively small to be easily implemented in networks

The second way to increase performance is the use of a double valve. This is 2 compliant valves as seen in Figure 2a on top of each other, with this setup the supply line is squeezed between the 2 control lines. A schematic can be found in Figure 2c

4.1.2 Normally closed valve

The previously discussed designs were always open valves, this valve is a normally closed valve (NC-valve). A working valve could provide other working logic schemes. Because this valve will function as a simple AND gate in Boolean logic, this would open up more possible logic networks. An example where this where could be used is the Zhu logic scheme see subsection 5.3. The dimensions of this valve would fit in an area of roughly 15x15x12 mm.

The cross-sectional area of the supply line is increased because generally, the pressure drop is related to the cross-sectional area. Increasing the area is achieved by inflating chambers on each side of the valve. By inflating the valve is lifted upwards and is opened, see Figure 3 and Figure 4.

More information of the analysis can be found in subsubsection 4.2.1, information about manufacturing in subsection 4.4.

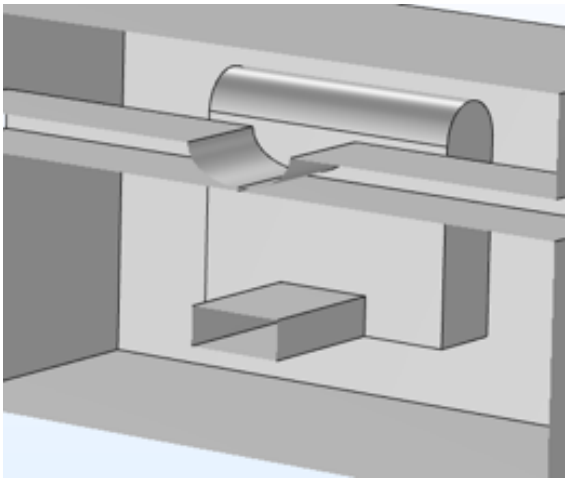

Figure 3: NC valve closed

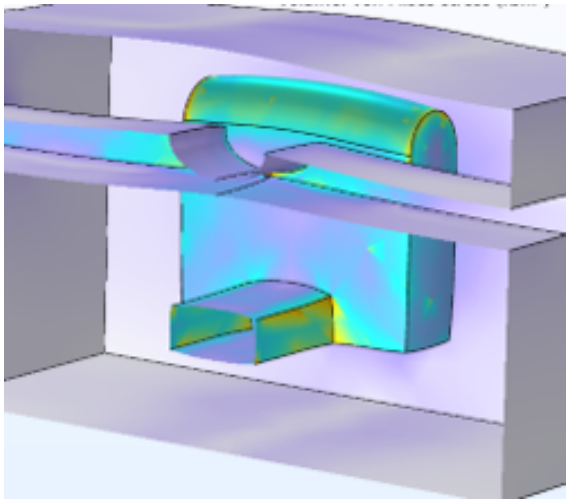

Figure 4: NC valve open

4.1.3 Demultiplexer

A demultiplexer is defined in this paper as a logic scheme where you can have more outputs than inputs. The logic components that are used in such a scheme are the valves discussed in this paper. What makes the demultiplexer of this paper unique is that it is fully compliant and uses water as a medium. Water is sparsely used in the field of soft robotics and compliant logic circuits are novel. Water also has the added benefit that is not compressible, this makes calculating volume simpler compared to pneumatic approach.

For controlling an array of actuators 2 possible control schemes can be used and explored. These schemes are based on other works and then changed so that they could work in a soft logic fluidic circuit.

One layout of the demultiplexer was originally based on the works from Bartlett *et al* [6], a schematic can be found of and 3 to 8 demultiplexer in Figure 5. N supply channels can be controlled with $log_2 n + 2$ rigid valves.

In line PC (power control) there is always a constant flow that is under a certain pressure, PC is the second named line see schematic. Due to the pressure in each of the 3 rows where PC is connected the compliant valves will close half of each supply line in each row, 1 non-zero output of the supply channel will remain. The compliant valves in this schematic are the parts where the channel is wider.

SC_i (signal control with index i) are channels that are controlled by a rigid valve, these are closed chambers inflated by adding fluid. When 1 of these compliant valves engages it will close half the supply channels in 1 row but also close the Pc channel in the row above, thus opening the supply channels that were originally closed. Now the original supply channel output is zero and a new one is now non-zero.

The second is based on the work done by Zhu *et al* [1], the scheme scales with N^2 outputs with $2N$ rigid valves. This scheme has a 2D array with columns and rows. The bottom lines(Cs_i) that have the default state of being always on will close all the internal soft valves of that columns. When output needs to be selected Cs_i has to be low and Rs_i has to be high, at the cross-section of this collom and row the actuator is powered. This scheme also allows the power of an entire row of actuators at once. A schematic can be seen in Figure 6

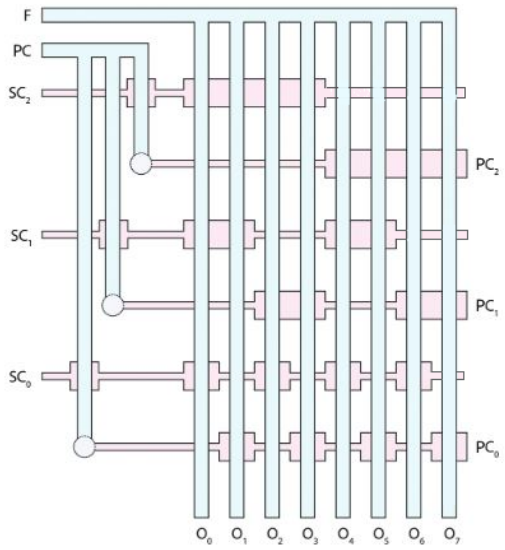

Figure 5: Barlet

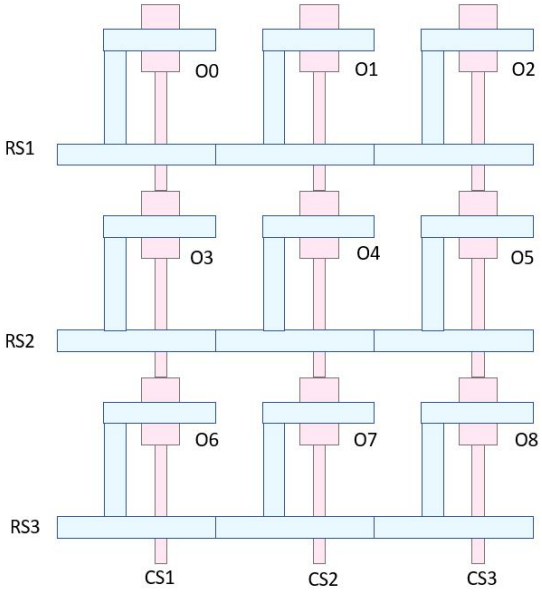

Figure 6: Zhu

One of the major differences is that Barlet *et al* [6] needs a valve that can close higher pressure differences, in the entire system there are 3 different pressures. The one by Barlet *et al* can only have 1 active output, the one of Zhu *et al* [1] is between 1 and the entire row.

4.2 Analysis

In this section information is given on the analytical approach of calculating the valve and demultiplexer. In subsubsection 4.2.1 information about the FEM simulations of the valves is found. In subsubsection 4.2.2 information is provided about the calculations of the demultiplexer using separate FEM Simulations and graphical program scripts.

4.2.1 FEM modeling valves

The key question for the valves is to know at what pressure the control line closes the supply line, in the case of the normally closed valve at what pressure does it open? In this section below the procedure explains both the modeling for the normally closed and normally open valve.

A model is built and FEM is used to calculate this due to being a more practical approach than doing it analytically. The section where the supply line and control line cross each other is modeled due to being the most relevant.

FEM simulation program COMSOL with the solid mechanic's module with the hyperelastic material package is used for modeling the material behavior. The Yeoh hyperelastic material model is used with the material constants found in the review paper of Xavier *Et al* [11].

Simulating a complete FEM model is omitted, only a simplified version has been done. The reasoning for this is that it would be difficult and time intensive for setting the correct boundary conditions for: fluid flow, fluid-structure interaction, contact surface interaction, time steps and modeling the structure to the fixed world. The simplifications will be mentioned in the text below. The quake valve, the 10x10 mm valve, and double valve were modeled as if the valve was fixed to the ground. FEM simulations for the rope-reinforced valve and multi-material valves are omitted due to time constraints.

For the valve, each fluid is modeled in each line as constant pressure, no moving fluid is modeled. The pressure in the control line is increased incrementally until the bottom of the supply line clips through the top of the supply line, as seen in Figure 7 and Figure 8, in the case of a normally closed valve when the valve is opened see Figure 10 and Figure 9 With this procedure, a good starting point was found when the valve is closed or opened with a significantly simplified model. Assuming that the pressure of the control line is constant is valid because there is only hydrostatic pressure. Due to this simplification, an error is introduced in the supply line, the pressure is now constant instead of a gradient that spans over the length of the valve. This error would overestimate pressure due to the constant pressure only having the highest value of the gradient.

Later a complete fluid network model is built as seen in subsubsection 4.2.2. For this model, a function is needed to capture the relation between the volume in the control line and the pressure in the control line in the normally open valve. The method of how this function is found will now be described. A channel was modeled in Comsol that is slowly inflating via the procedure mentioned earlier. Volumetric deformation and control line pressure was measured and via a parametric sweep these data points were collected. The data points are then fitted using the Matlab tool fitting toolbox. A power function was used to fit data because it described the data the best, this procedure gave the following fitted function $P = a * V^b$. P is the pressure in the supply line and V volume, a ($1.08 * 10^8$ [$N/m^{3.7577}$]) and b(0.5859 [-]) are fitted constants.

For the complete fluid network model discussed in subsubsection 4.2.2 a relation between the control line pressure and flow through the supply line is needed. This section describes how this is achieved, at a certain pressure, the complainant's valves will start to operate. When this happens the valve slowly closes thus the flow of the supply line slowly goes down because the hydraulic resistance goes up. Equation 1 captures this behavior, the shape of the function was found empirically when testing the valves see subsection 4.3. c_1 (30 [N/m^2]) c_2(3.5 [-]) and c_3 (1 [m^2/N]) are fitted constants p is the pressure in the control line. This function always has a value between 1 and 0. When p is between 0 and 25 kPa f is roughly 1, when p is 35 kPa, it approaches zero. The pressures mentioned earlier are found empirical when experimenting with the valves, for more information see subsection 4.3

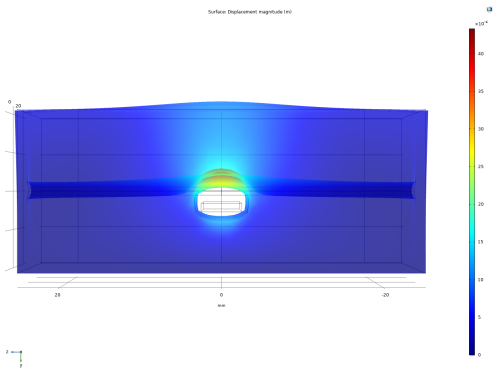

Figure 7: Normally open valve closed

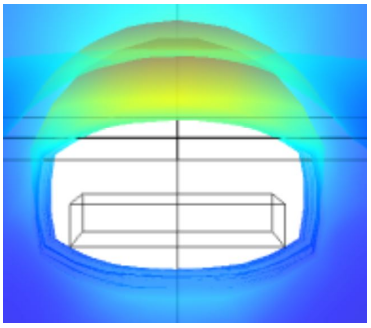

Figure 8: Normally open valve closed zoom into valve to section

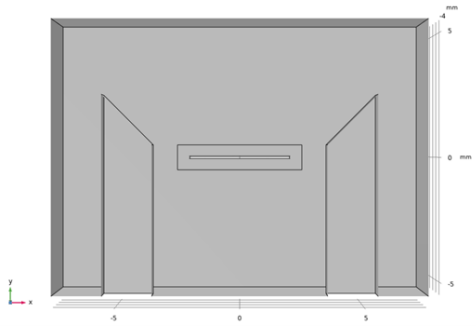

Figure 9: NC valve off

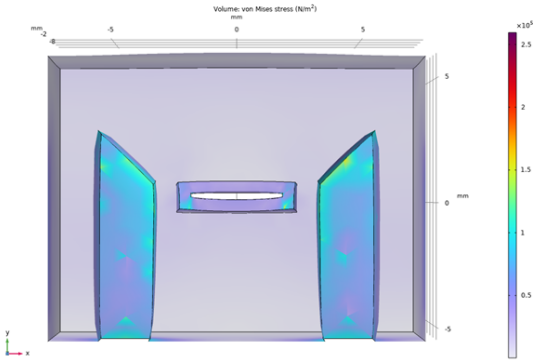

Figure 10: NC valve on

4.2.2 Simulation demultiplexer

The objective of the simulation is to calculate the bandwidth of the demultiplexer.

Simulating complete FEM simulations is omitted due to the limited available computer power.

For that reason, a simplified model was created in Matlab Simulink. The Simulink model consists of multiple custom blocks, these blocks capture the behavior of the valves.

The smaller components(valves, lines, etc) are modeled in FEM models and simulated separately from the Simulink model for information see subsubsection 4.2.1.

4.2.2.1 Complete model

In Figure 11 the complete simulation model can be seen. It starts in the left top light blue square where the first pump is located, volumetric flow to the actuators starts here through 8 supply lines. The 8 supply lines go into the middle top green square where they go into a series of product blocks that multiply by a value named f that is between 0 and 1, a product block multiplies f with the volumetric flow. The values f are calculated in the bottom dark blue or red blocks see Figure 11. These blocks represent the compliant valves, more information about these blocks is found in paragraph 4.2.2.3 and 4.2.2.2. At the right side of the green square, 1 supply line will be non-zero and goes into the orange square in this block the time it takes for the fluid is taken into account for more information see paragraph 4.2.2.4. Then goes to the top right purple square. Here are the blocks of the actuators more information can be found in paragraph 4.2.2.6.

Digital signal generation starts in the bottom left yellow corner(see Figure 11) where a signal is sent to the rigid valve to open or close. Information on the valve can be found in paragraph 4.2.2.5. After the rigid

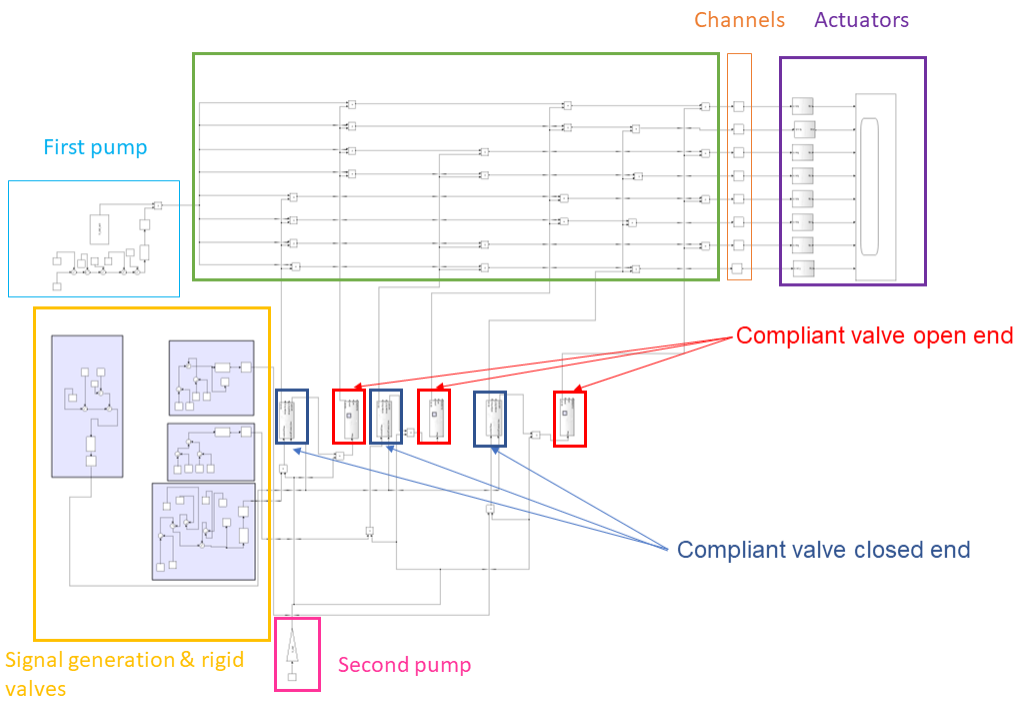

Figure 11: Complete model demultiplexer

valve a 1 or 0 signal is sent to a product block, where it is multiplied by a second volumetric flow value, and the second pump is located in the bottom pink square. After that, the output of the product block goes to the open-ended compliant valve section located in the dark blue square, again see paragraph 4.2.2.2. When the pressure reaches a certain threshold f will be zero. When the pressure reaches a higher threshold the compliant valve open end would be closed off.

4.2.2.2 Compliant valve closed end

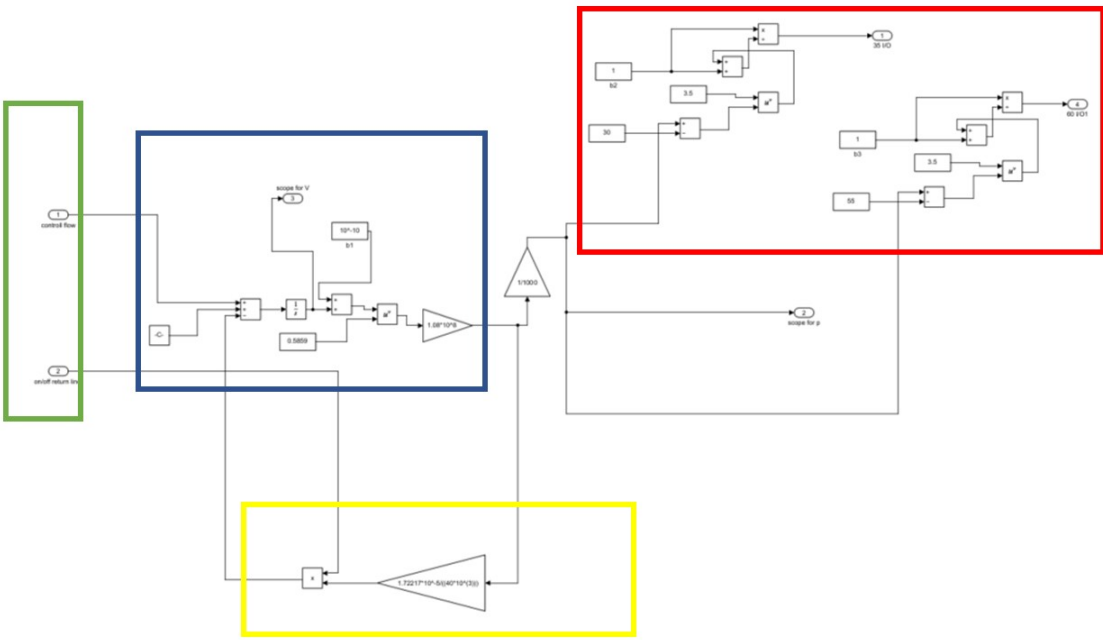

Figure 12: Simulink model Compliant valve closed end

1 control channel operates 4 compliant valves. The soft compliant valve is operated by increasing the pressure on the control side. 1 side of the channel is used to add fluid, the other one is closed by a rigid that can open and close to discharge the fluid. This section first describes inflating of this control channel after that the discharge of a control channel.

These simulations start with volumetric inflow. That is the top block in the green border block, as seen in Figure 12. After that, the volumetric flow goes to the dark blue square in Figure 12 where the volumetric flow is integrated to get volume. From the volume in the channel, the pressure is calculated based on equation $P = a * V^b$. From the pressure value f is calculated, more information about f is given below.

At a certain pressure, the complainant's valves will start to operate. When this happens the valve slowly closes thus the flow slowly goes down because the fluidic resistance goes up. The shape of the flow control pressure was found empirically, Equation 1 captures this behavior. c_1 (30 [N/m^2]) c_2(3.5 [-]) and c_3 (1 [m^2/N]) are fitted constants p is the pressure in the valve, c_3 is used to make the exponent dimensionless. This function always has a value between 1 and 0. Between 0 and 25 kPa it is roughly 1, above a 35 kPa threshold, it approaches zero.

These calculations are done in the top right-red corner. The output of this function is later multiplied with the volumetric flow that goes to the actuators, this is outside of this function block. The signal to close the open-ended tube is also calculated there. More information about the open-ended tube is in the next paragraph

$$f = \frac{1}{1 + c_2^{((p-c_1)/c_3)}} \tag{1}$$

The volume that has been accumulated also needs to discharge. This section will give more information about this. When discharging needs to start a 1 signal is sent from the bottom block of the green square again see Figure 12, when this signal is 1 calculation of the outflow are started. It is assumed that the outflow is linearly proportional to the pressure, as the equation $\dot{V} = K * P$. The reason for this there is a literature gap on how to calculate this. K is defined experimentally, by inflating a silicone tube and looking

at the time of discharge. These calculations are done in the yellow bottom square see Figure 12.

4.2.2.3 Compliant valve open end

The compliant valve open end is almost the same as the valve closed end as discussed previously. The only difference is that there is now constant outflow.

A constant flow of fluid generates pressure that blocks the flow in the control line at a pressure of 35 kPa, at this pressure the normally open valve is engaged and stops the flow in the supply line. Because the valve is open-ended there is the constant volume in and outflow. An orifice that restricts flow is placed at the end of the tube. This creates some extra volume in the tube. The outflow is modeled as a $V_{out} = c * \sqrt[2]{P}$. This is based on a ISO standard [12] of a known orifice plate, as seen in Equation 2. P is the pressure, c is a constant selected that the pressure converges in a steady state of 40 kPa. In constant c all relevant constants of the orifice plate are captured (eg C_d, ϵ, ect). The volume in the control line is is know by integrating the flow of the channel, this is done with the same method discussed in paragraph 4.2.2.2.

$$\dot{V} = \frac{C_d}{\sqrt{1-\beta^4}} \epsilon \frac{\pi}{4} d^2 \sqrt{2\Delta p * \rho_1} \tag{2}$$

All the open-ended and closed-ended valves located in the dark blue and red squares mirror the logic component inverter AND gate that are chained together as seen in Figure 13. A minimum 1 AND gate is needed to capture the logic of the normally open valve, but it is possible to add multiple AND gates to the output of the Inverter block.

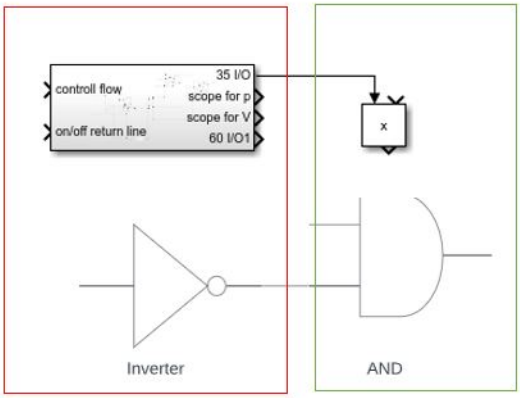

Figure 13: Logic compersion Simulink blocks

4.2.2.4 Channel

It is relevant to capture the time required for the flow to reach the actuators. To model this a time delay block is put in front of the actuators. The time delay is calculated according to this equation $t = (A_{cros})/(L * \dot{v})$. A_{cros} is the cross-sectional area of the channel, a quick check with a FEM simulation showed that deformation is small roughly 5,3 mm^2, the deformation is caused by fluid flow through the compliant channel. For that reason it will be set constant. L is the length of the channel. $\dot{V}$ volumetric flow entering the channel from the earlier remains constant.

4.2.2.5 Rigid valves

The rigid valves are modeled as a time delay of 100 ms, this value was given by the manufacturer. A lowpass filter of 10 hertz is added in front of the delay to block frequencies the valve can not follow. The 10 hertz is based on the switching speed of the actuator. The electric signal of the controller to the valve is modeled as instantaneous, the time delay of the electric signal is insignificant compared to the volumetric flow.

4.2.2.6 Actuator

An actuator has been simulated in Comsol, the design was based on the work of a previous thesis from another master student. The valve is relatively small the internal volume is 535 mm^3 while not inflated. A fit is made with the volume and stroke, this relation is linear. S is the stroke of the actuator, V˙actuator is the added volume, C($3 * 10^6$) is a fitted constant. The added volume is calculated by integrating the volumetric flow over time.

$$s = C * V_{actuator} \tag{3}$$

4.3 Experimental setup

This section provides information about the experimental setup of the: normally open, normally closed and demultiplexer.

Experimental setup valve

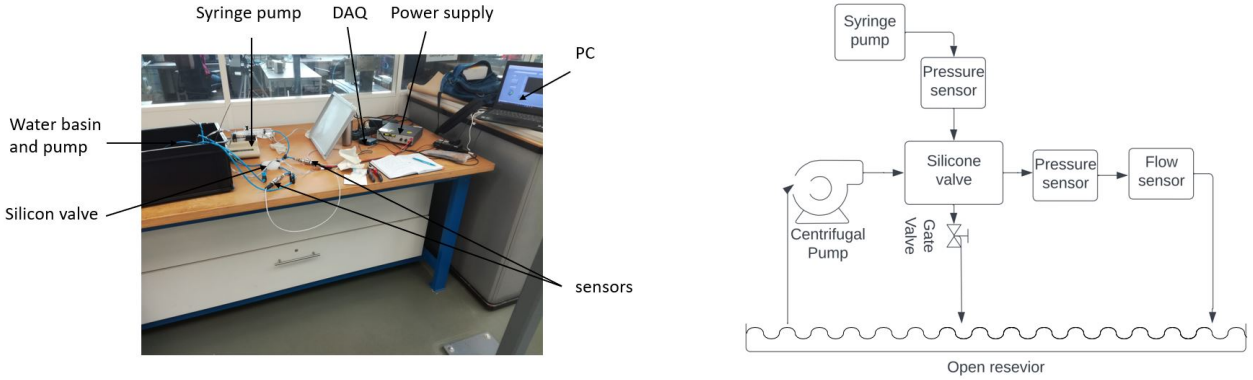

(a) Experimental setup normaly open valve

(b) Schematic compliant valve normally open

Figure 14: Experimental setup NO valves

The goal of the experiments is to find the closing pressure of the supply line. This is achieved by measuring the pressures of the supply and control line. The flow of the supply line is also captured, this is needed to check whether the flow is zero and can be also used to calculate the hydraulic power loss.
A pump that is connected to a controllable power supply generates a pressure and flow of 12 kPa and 1.3 L/min and is connected to the supply line of the valve via a hose as seen in Figure 14a and Figure 14b, these are the starting values of the experiment. After the supply line, a pressure sensor is connected after the pressure sensor a flow sensor is connected. After that, the line returns to the reservoir where the pump is located.

The pressure of the control line is increased by slowly inflating that line with a syringe pump with a constant flow rate of rate(427.1 ml/h). This pump is connected to a pressure sensor(Telemecanique-XMLP500MD71F). After the pressure sensor, the line is connected to the control line. At the end of the control line there is a rigid shut-of valve that is closed during experimenting. When the experiment is complete the rigid shut-of valve is opened and the water is discharged into the reservoir.

The pressure sensors and the flow sensor have their own DAQ (data acquisition) systems. These 2 DAQs are connected to a laptop to capture the data.
The experiment is started by turning the pump on after that that the syringe pump is started. The experiment ends when the pressure of the control line is between 45 to 50 kPa or if the pressure of the supply line is zero, the reason for this is that 50 kPa is the maximum measuring range from the sensor. If an experiment needs to be done that goes outside the 50 kPa range an analog gauge is used. The gauge is placed at the

same location of the digital gauge and pressures are noted down at different intervals.

To experiment with different boundary conditions additional experiments are performed with an altered valve. Alterations include: tiewraps, fixed top bottom, or all walls fixed. All this test were conducted with the compliant quake test as seen in Figure 2a

For 1 additional experiment tie wraps were placed around the valve, as seen in Figure 15a. 3 experiments were conducted to see how the tightness of tiewraps changes the performance of a quake valve. In experiment 1 the tiewraps are loose around the valve. In experiment 2 followed the surface of the valve, but was not tight. Experiment 3 was very tight, it was clear to see that the valve was deforming due to the tiewraps. The tiewrap was selected due to ease of implementation.

For the second additional experiment, the top and bottom were fixed using 2 wooden panels and adjusting screws as seen in Figure 15b, note that the "plates" were planes placed just above the valve with clearance to prevent pre-tension.

For the third additional experiment, the walls were all fixated. Fixating all the walls was done by 3D-printing a "cage" that surrounds that valve, to prevent pre-tension there was clearance given to the walls as seen in Figure 15c.

To get an understanding of the hydraulic performance of the valve the hydraulic power loss is also calculated. This is done by measuring the volumetric flow and pressure of the supply line. The valve selected is the compliant quake valve.

It is interesting to know how the valves perform with higher pressure, specifically pressures high enough to close other control channels. The max pressure to operate is selected to be 100 kPa, otherwise the pressure would be unpractical high The reason for this is that it enables more complicated fluidic logic circuits. This will be done by selecting and combining the best-performing valve designs and boundary conditions that are described above.

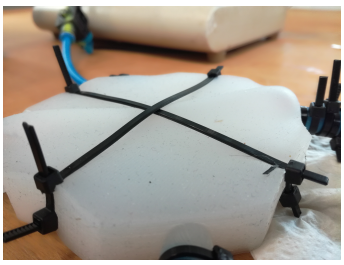

(a) Tiewraps

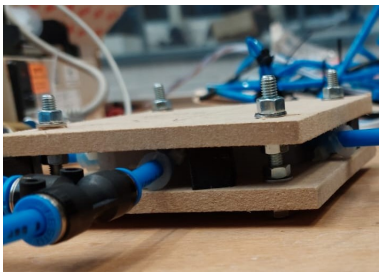

(b) Plates

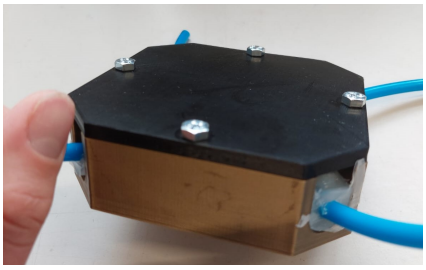

(c) Cage

Figure 15: section different valves

Normally closed valve

The purpose of this experiment is to find the relation between the pressure drop of the supply line in relation of the pressure in the control line.

This is achieved by measuring the pressure before and after the valve, and the pressure of the control line.

A pump is connected to the supply line of the normally closed valve and is connected to a pressure sensor, then to the normally closed valve.

Using a manual quench valve the starting pressure in the supply line is set to 12,5 kPa. The sensors are placed before and after the valve to measure the pressure drop over the valve. The control line is slowly filling up with a syringe pump. The pressure is monitored using an analog gauge, a schematic and picture

can be found in Figure 16.

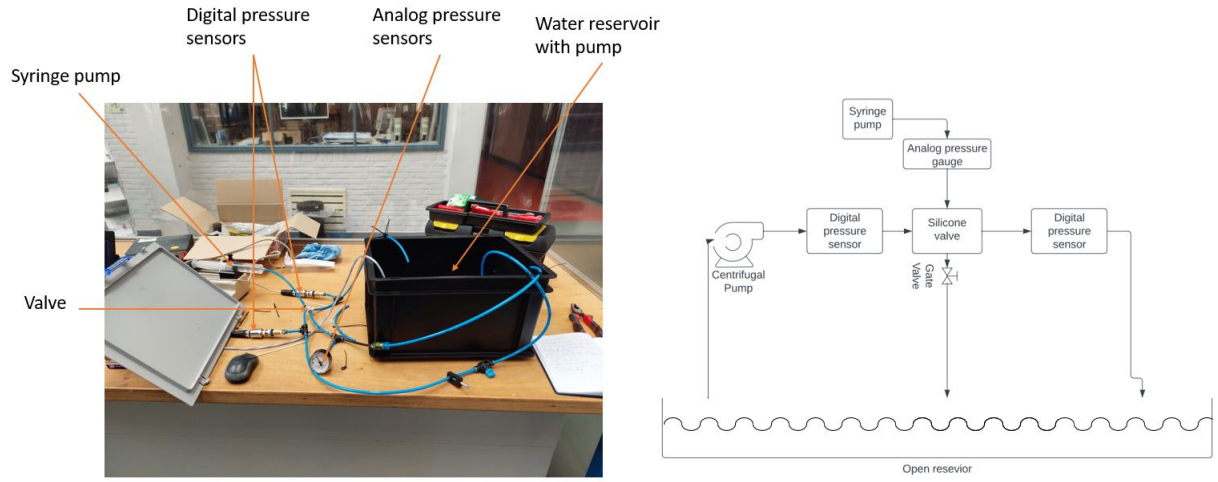

(a) Experimental normally closed valve setup

(b) Schematic normally closed valve setup

Figure 16: NC experiment setup

Experimental setup demultiplexer

The aim of this experiment is to find the maximum switching frequency of the demultiplexer. This is measured by 3 flow sensors, based on the time difference when sensor 1 detects no flow and when sensor 2 detects flow a frequency is estimated. A schematic overview can be found in Figure 17, with a picture of the physical setup. Operating the demultiplexer is done by activating rigid valves S0, S1, S2 in an specific combination.

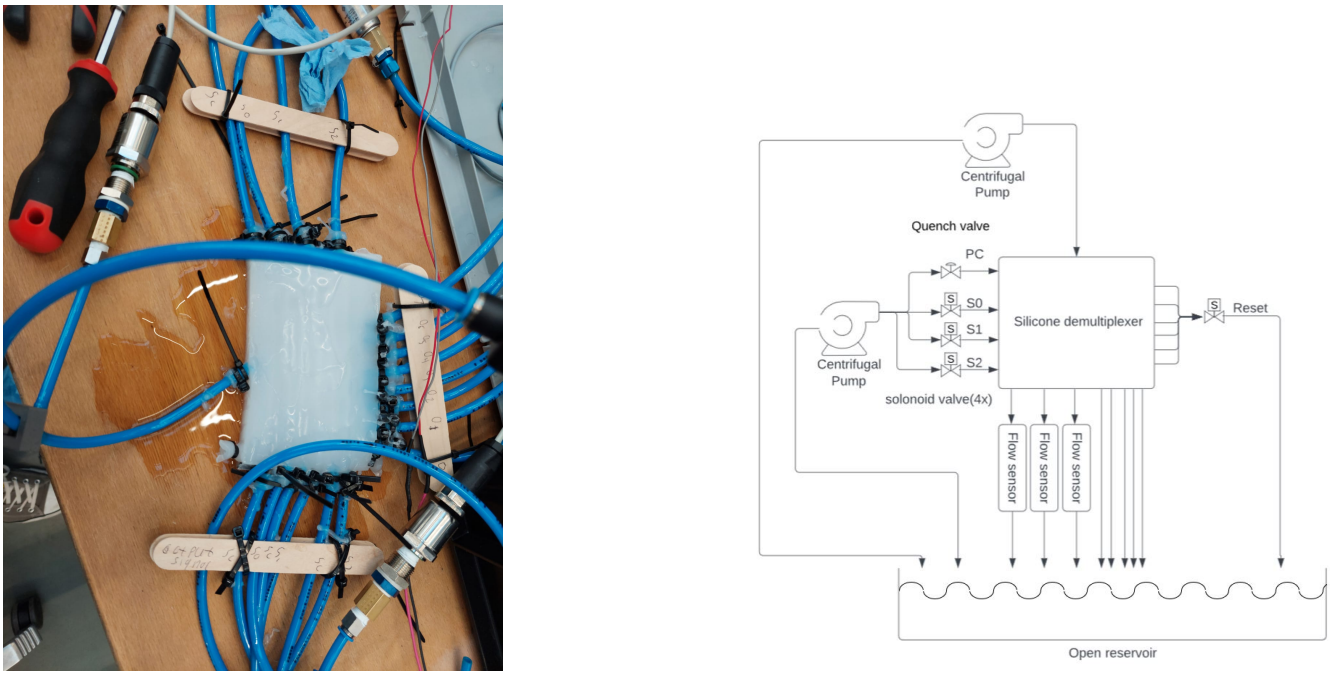

(a) Experimetal setup demultiplexer

(b) Schematic experiment setup demultiplexer

Figure 17: Experimetal setup demultiplexer

4.4 Manufacturing

In this section information is given about the manufacturing of the prototypes. In subsubsection 4.4.1 information is found about building the normally open and closed valves. Information about the demultiplexer is found in subsubsection 4.4.2

4.4.1 Manufacturing valve

Fabrication of the valves was done by 3D printing a mold of PLA (Polylactic acid) and inserts of PLA or PVA (PolyVinyl Alcohol). The PVA is water-soluble and is thus used in different valves where the lost core method is applicable. These inserts are laid inside the mold and fixed inside by blockers. A 3D-printed round sleeve of PVA is put on the insert by clamping them down by a blocker that is fixed by bolts, see Figure 18a. When the mold is fully prepared the mold release is sprayed and silicone is cast, an overview of the mold can be seen in Figure 19. The hoses are fixed to the valve with the use of tie-wraps and cast nipples that are formed by the mold, as seen in Figure 19. The PLA inserts are removed by hand by wiggling or pulling. The silicone part with PVA inserts are put in a heated ultrasonic cleaner for a couple of hours and put in water overnight, after these operations the inserts were partly dissolved. After that, the inserts were flushed out with a pump with a low volumetric flow.

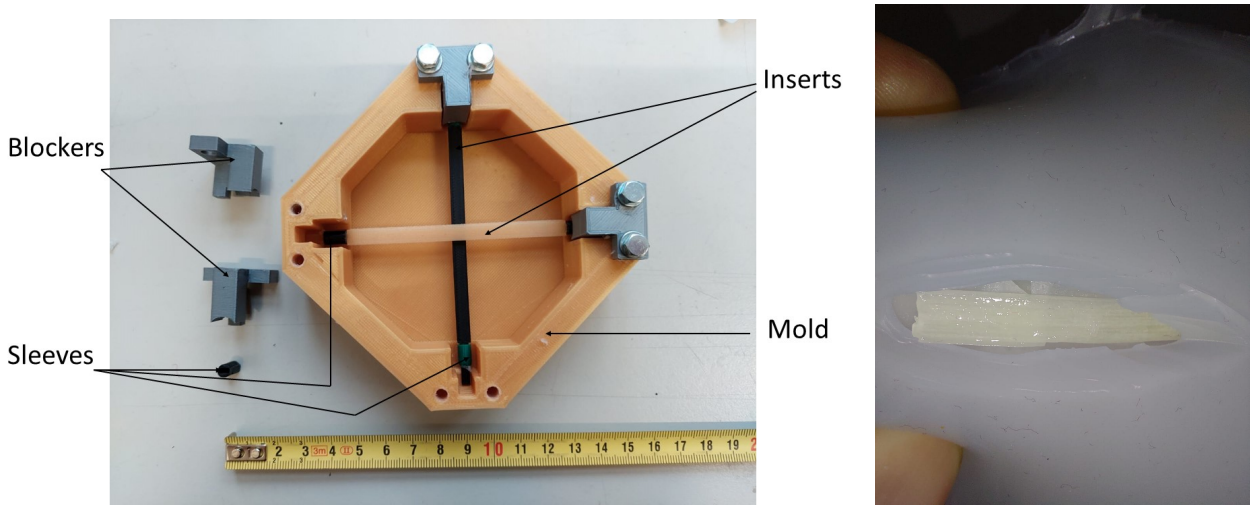

(a) Mold normaly open valve

(b) Repairing double valve

Figure 18: Manufacturing and repairing double valve

Figure 19: Hose connection

The same mold used in a mono-material valve is also used in a multi-material valve. Manufacturing was done by pouring, waiting for it to set but not fully cure, and then pour the next layer.

This process is recommended by the manufacturer (Smooth-on). In Table 1 a summary can be found of the attempts made. The bottom layer was cast to the height of the first insert. The middle was between the

top of the first insert and the bottom of the second insert, this layer became the membrane between the 2 channels. The top layer was cast to a height that made the entire stack roughly 13 mm.

For the middle layer where the membrane is located Ecoflex-0010 is used, for the top and bottom Ecoflex-0050 or dragon skin 10 medium are used, these materials are roughly 1.5 and 10,75 times stiffer than Ecoflex-0010 at 100 % extension. These materials are selected due to the availability and abundance of literature about them. The E modulus of 0 % extension was hard to find for both materials however up to 100 % extension both materials have an approximate linear stress-strain curve so the E modules at lower extensions are roughly the same.

Trail	Materials	hours between layer 1 and 2	hours between layer 2 and 3
1	Dragonskin 10/Ecoflex-0010/Dragonskin 10	5	4
2	Dragonskin 10/Ecoflex-0010/Dragonskin 10	1,15	1,2
3	Dragonskin 10/Ecoflex-0010/Dragonskin 10	3	3
4	Dragonskin 10/Ecoflex-0010/Dragonskin 10	3	3
5	Ecoflex0050/Ecoflex0010/Ecoflex0050	3	3
6	Ecoflex0050/Ecoflex0010/Ecoflex0050	1	1

Table 1: Curing times multi materials

Repairing a damaged valve is also possible. This is demonstrated by fixing the most geometric complex valve, the double valve as seen in Figure 18b. Repairing is achieved by making an incision where the valve is damaged. The next step is putting inserts back in, this was done by inserting one of the original inserts back in via the supply line, this insert was modified by cutting one half making it "y" shaped to allow insertion. The following part is to apply silicone at the damaged area and the walls of the incision. After letting the silicon cure overnight the insert was manually removed.

4.4.2 Manufacturing demultiplexer

The demultiplexer has been selected for building and experimentation, design of the logic circuit is discussed in subsubsection 4.1.3. The 2D demultiplexer based on Zhu *et al* has not been implemented due to time constraints. The compliant quake valve, see Figure 2a has been implemented into the demultiplexer. The other valves were designed in a later stadium.

For the demultiplexer, a mold was 3D printed as seen in Figure 20a. The inserts are made of PVA for the use of the lost core method.

These inserts are clamped down at the inlet and outlet locations. Clamping down was done with "blockers" that are in turn fixed with bolts.

After the mold is assembled Ecoflex00-50 is cast. Ecoflex00-50 was selected due to having the best performance for a single material valve as discussed in section 5. After casting the inserts needs to be dissolved, the same steps were used as discussed in subsubsection 4.4.1.

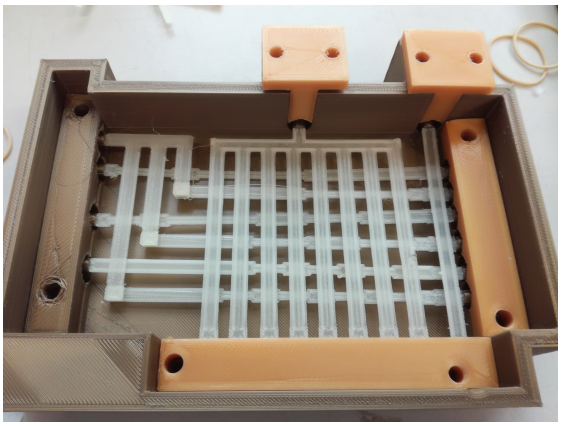

(a) Mold silicone demultiplexer

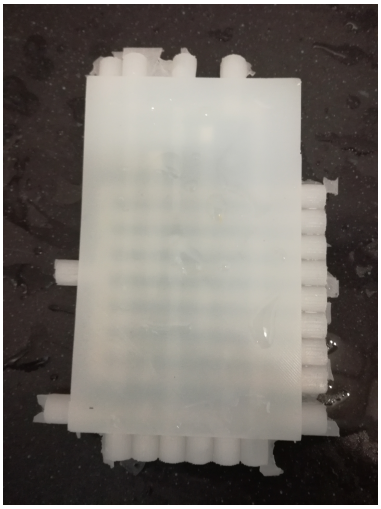

(b) silicone demultiplexer

Figure 20: silicone demultiplexer

5 Results

In this section, results are presented. In subsection 5.1 the results of the compliant valves can be found. The results of the normally closed valve are presented in subsection 5.2. Performance of the demultiplexer has been discussed In subsection 5.3.

5.1 Compliant quake valve

The experiments are conducted as described in section subsection 4.3 and the results are shown. What is shown is how the pressure in the supply line(y-axis) decreases due to inflating of the control line (x-axis). Results gathered from FEM analysis as discussed in subsubsection 4.2.1 are plotted as a vertical line in the relevant graph, this line is where the valve is closed according to the FEM simulations.

It has to be noted that every graph of a valve has 2.15 kPa subtracted. This is due to pressure that is created by a water column by lifting the hose 22 cm up to the reservoir. It is assumed that the water column spans the entire height due to the flow of the supply line going slowly to zero due to the slow inflating of the control line. 1,13 kPa offset is added to the supply line, this is needed to account for the pressure drop of the fluid moving through the hose from the silicon valve to the pressure sensor. This offset is calculated by taking the average hose length between the valve and sensor (7.57 [cm]) and multiplying it with the pressure drop(0,15 [kPa/cm]) that is found in a separate experiment. After these operations the results are normalized by dividing by 11,5, this was the starting pressure after the previous operations. Each test has been repeated 5 times.

Multilayered valves were prone to delimitation in the control line in the corner. Due to this only one experiment could be properly conducted before the valve was damaged. The results can be found in Figure 22.

The 3 designs(quake valve,10x10 mm valve, and double valve) are discussed in subsubsection 4.1.1 and are plotted in the same graph so it is easy to compare them. The graph can be seen in Figure 21

In subsubsection 4.4.1 it was mentioned that a double valve was damaged and then repaired. The results of the repaired double valve can be found in Figure 25. In subsection 4.3 it was explained that 3 methods (plates, caged and tiewraps) were used to rigidly reinforce a quake valve. The results found with the rigid reinforce valve can be found in Figure 23.

The hydraulic performance of a quake valve can be found in Figure 26.

In subsection 4.3 it is explained that there was a separate test done with the trip test with different tensions. The results of the tiewrap test can be found in Figure 24.

The results of the double valve and quake valve operating at higher pressure can be found in Figure 27 and Figure 28. These tests were conducted with plate boundary conditions, otherwise, the control pressure would be unpractical high(plus 1 bar). The starting pressures are selected based on the converging pressure of closing the valve at 12 kPa pressure of the supply line. For the Quake valve 1 test is plotted for readability, each test looked similar to the other.

In order to give a good overview of the key information Table 2 is made. Here it is noted when the pressure starts to go down(pressure start choking), and also noted at what pressure of the control line the pressure in the supply line has converged(pressure closing).

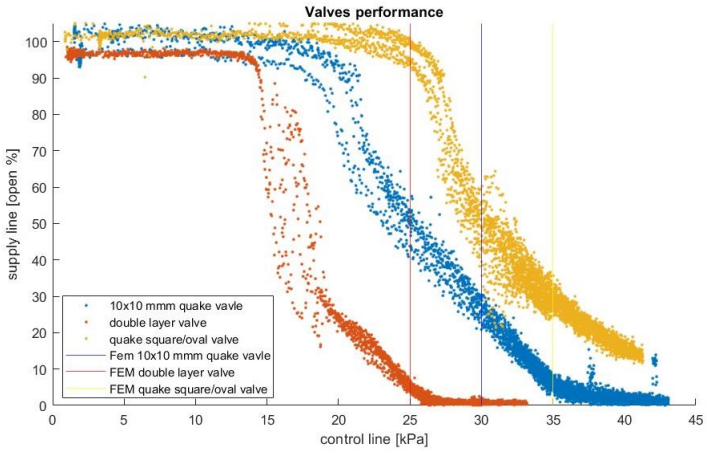

Figure 21: Quake , 10x10mm and Double valves, material ecoflex-0050

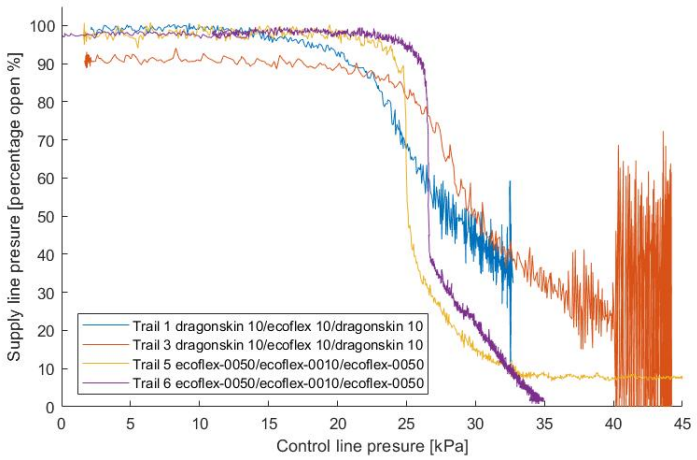

Figure 22: Quake valve with diffrent combinations of materials

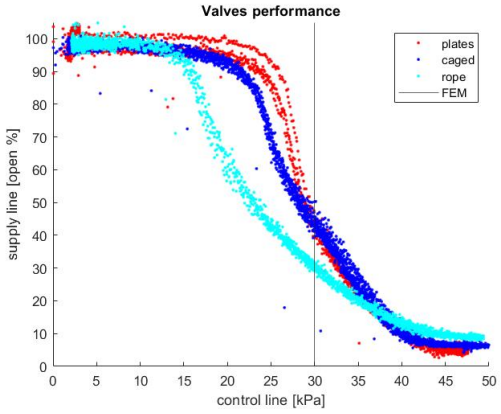

Figure 23: quake valve that is reinforced with: plates,caged or tieraps

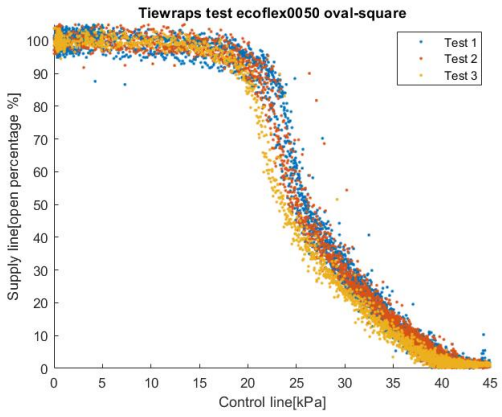

Figure 24: Test tie wraps with different tensions

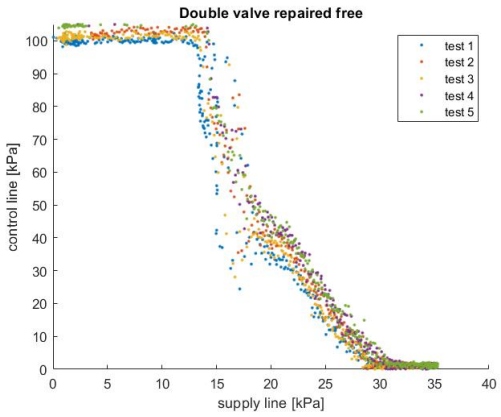

Figure 25: repaired double valve

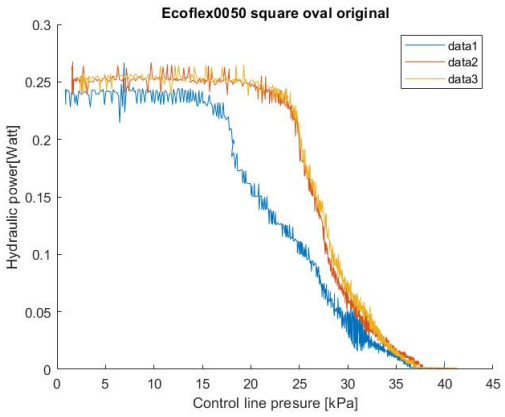

Figure 26: Hydraulic performance quake valve

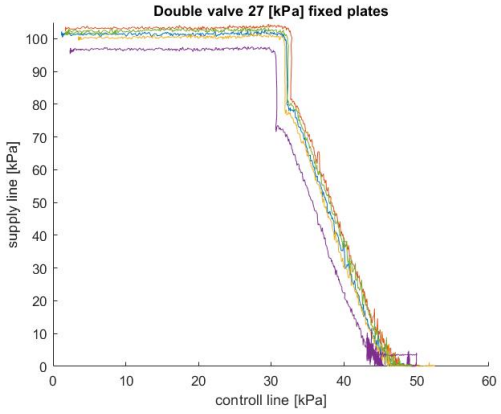

Figure 27: Double valve 27 kPa

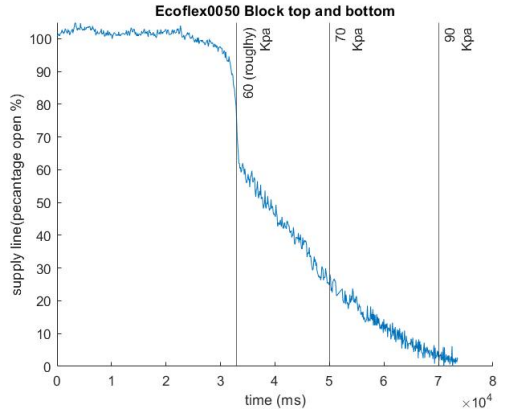

Figure 28: 35 kPa quake valve

			12 [kPa]	
shape valve	**material**	**misc**	**presure start choking [kPa]**	**presure closing [kPa]**
sq x sq	eco0050	x	36	46
sq x oval	eco0050	x	25	40
10x10 vavle sq x oval	eco0050	x	20	35
double sq x oval x sq	eco0050	x	15	30
10x10 vavle sq x oval	eco0050	tie rips (2e trail)	15	33
sq x oval	eco0050	bound in rope	15	45
sq x oval	eco0050	blocked top&bottem	25	45
sq x oval	eco0050	caged	20	40
sq x oval	eco0050	tie rips (2e trail)	20	40
sq x oval	dragon10/eco-0010/dragon10	multi material	20	Not found
sq x oval	dragon10/eco-0010/dragon11	multi material	25	Not found
sq x oval	eco0050/eco-0010/eco0050	multi material	25	35
sq x oval	eco0050/eco-0010/eco0050	multi material	26	35(?)

Table 2: recap result valves

5.2 Normally closed valve

The experiment has been conducted according to subsection 4.3. These results can be seen in Figure 29. The pressure before and after the valve was subtracted from the other, as seen on the y-axis. performance of

the normally closed valve is defined as the lower the better. Accurately plotting the pressure in the control line was not achieved due to the digital pressure sensors can only measure up to 50 kPa. On the x-axis, the added volume in the control line is plotted. The vertical lines are the pressures found on the analog gauge at that particular volume. The pressure difference did drop. This was due to expanding of the crossection of the valve, but at roughly 40 kPa the pressure difference increased quickly.

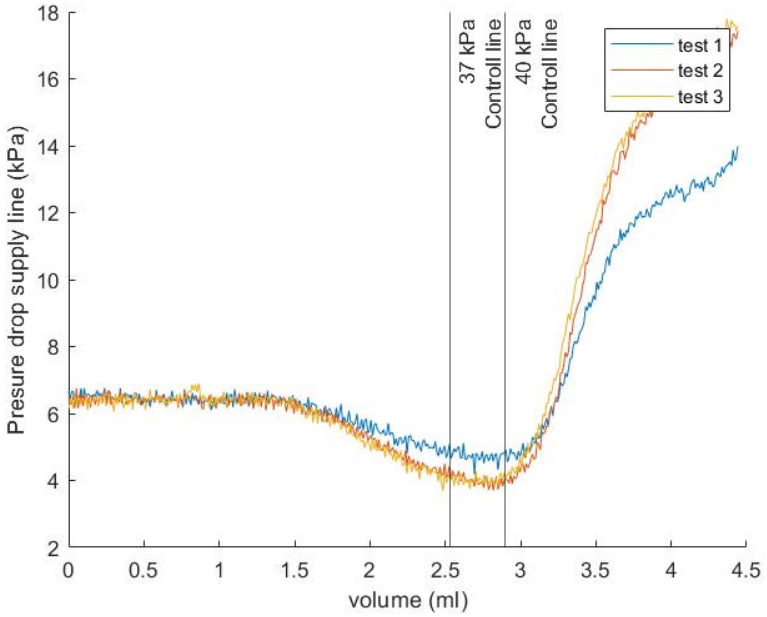

Figure 29: NC valve on

5.3 Demuliplexer

The Simulink results can be found in Figure 30. Details about this simulation can be seen in subsubsection 4.2.2. The switching speed from the demultiplexer is what is measured in this simulation. What was simulated was powering an entire array of 8 actuators, each actuator went from 0 to 5 mm stroke. The internal volume of an actuator while not inflated is 535 mm^3.

The signal to generate this pattern was done by hand by incrementally changing the time, this method was quicker than deriving a formula. It takes roughly 2,4 seconds to refresh an array of 8 actuators. One actuator takes 0.25 seconds. Resetting the signal lines takes 0,3 seconds.

The original goal of the experiment was to find the switching speed between 2 outputs, as discussed in subsection 4.3. A completely functional demultiplexer was not achieved. After testing the demultiplexer was opened and an internal leak was found that connected 2 lines with each other. The leak significantly reduces the functionality of the demultiplexer, because the valve 1 supply channels that should be closed gain a little extra flow and the valve can not generate enough pressure due to the internal leak.

The functionality that was achieved was some 3 lines closed and opened with the signals provided by the control line. One thing to note is that the demultiplexer expanded in-plane direction. In total, the demultiplexer has 27 valves, with 1 valve not working which means that these valves have a manufacturing failure rate of $3,7\%$.

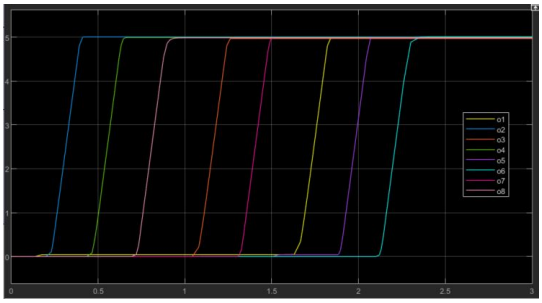

Figure 30: Y-axis stroke actuatro in mm, x-asxis time in sec

6 Discusion

In this section, a discussion will be held on the paper. Overall the main contrition of this paper is that the valves presented are manufacturable by hand and operate on a smaller scale than other compliant valves in literature.

Compliant quake valve
The valve designs in this paper are smaller than the average fully compliant valves. The valves in this paper are in the mm range while other valves in the literature are in the cm range. The results of multi-material valves are really promising for a valve that needs less pressure difference to operate when the technical limitation of delamination is solved. It has to be noted that the starting points delamination coincides with the stress peaks in the FEM model.

The results of the double valve design in this paper have some unexpected effects. The double oscillations in the double valve are in all likelihood created by "setting/or temporary oscillations of the membranes. This is in all likely hood the point where the membranes are starting to close the supply line.

NC valve
A possible reason for the steep rise in pressure is that the valve will deform in a way that negatively influences the performance of the valve which is not predicted in the FEM model. This design is quite novel, there is not a lot of research done for a fully compliant normally closed valve on this scale.

7 Conclusion

The main goal of the paper is to create a fully compliant fluidic network that is scalable, With scalable meaning that it can be used in large networks. To achieve this 3 different complaint valves were designed and simulated that are later used to build a fully compliant demultiplexer. The goal of the simulations was to find the pressure where the valves is closed. Experimentation verified at the wish point the valve was completely closed. The goal of the simulations of the demultiplexer was to find the bandwith experimentation to verify this result.

The FEM results showed that the closing pressure of the first valve is 35 kPa. The second valve looks the same as the first valve but had an increased area of 10x10 mm by the control line where the 2 channels intersect, its closing pressure is 30 kPa. The third design has 2 control lines above and under the supply line, its closing pressure is 25 kPa. The experiments of the valves matched roughly with the FEM simulations with a small overestimation. The result first valve was 45 Kpa. The second valve with a bigger area 36 kPa. For the third valve with 2 lines had a closing pressure of 27 kPa. It is also shown in the paper that repairing these vavles is possible making this a more valid approach for large-scale networks.

It was shown in the simulation of the demultiplexer that an array of 8 actuators took roughly 2.4 seconds to fully inflate. This method of simulating provided a computational lightweight while also being scalable

for larger logic circuits. A full silicone demultiplexer was built but did not function properly, due to manufacturing issues. Another could not be built due to time constraints. Even when the prototype did not function due to manufacturing it was 1 out of 27 valves that failed, that is 3.7%. The failure percentage would go down with more refinement of the procedure.

To answer the main question of this paper a fully functioning compliant demultiplexer has been built and experimentally studied, but due is prone to failure due to manufacturing errors. The valves that were designed in this thesis for this demultiplexer have dimensions in the mm range instead of the cm range that is found in the literature, it was also demonstrated in this thesis that these valves were repairable. These valves are also easy to manufacture. It could be said that this thesis has laid a good foundation for further improvement off the creation of a scalable solution for an actuating surface.

8 Recommendations

This thesis presents a couple of recommendations for future works.

Valves

Exploring the reason for the sudden increase in pressure in the normally closed valve could help improve the performance of the normally closed valve. The normally closed valve could open up more logic schemes.

It is shown that the use of different compliant and rigid materials (Eg rope, cloth, wire) could significantly reduce the required pressure difference for operating the valve while the entire valve remains compliant. This was not explored further due to time constraints. Solving the delamination problem could significantly reduce the required pressure difference. A possible solution for this is to cast an extra layer to bound layers.

Demultiplexer

It could provide benefits to build a new demultiplexer prototype to check whether the Simulink model matches the results.

Another improvement for the demultiplexer is the use of faster rigid valves that power the demultiplexer externally. This could help performance because these valves were a bottleneck during the simulations.

Some improvements in the experimental setup are required. A revision of the old scheme can be found Figure 31. Mayor changes are that the 3 control lines are connected to 1 rigid valve. Also, the actively controlled lines now have a check valve to prevent any back flow. The second major change is that there is a rigid valve at the end of the pump that provides tighter tolerances to reach the desired stroke. Without it it is possible that some overshoot would occur when the demultiplexer is discharging (resetting) its control lines.

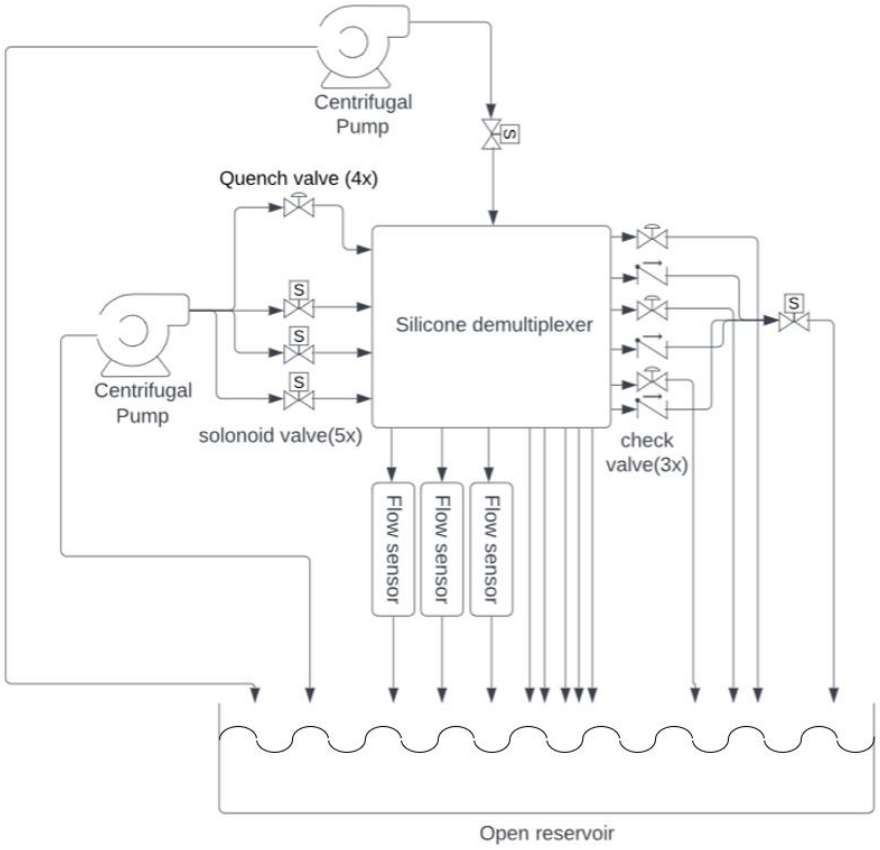

Figure 31: Improved test setup demutiplexer

Simulations

The FEM simulations of the normally open valves systematically underestimate the closing pressure. However, it has to be noted that this gives a good first insight with minimum effort. A weakness in the FEM model is that no flow is modeled. A model with all the required boundary conditions could provide more insights into the pressure loss effect and give better information on how to improve the designs.

Experimentation shows that there was a sudden increase in pressure drop in the normally closed valve. Modeling fluid flow in the simulations of the NC valve could explain why this is happening.

Manufacturing valves and demultiplexer

Building prototypes were done by making 3D printed mold and inserts, this process is cumbersome and has limited accuracy. Using silicone printing machines could provide tighter tolerances valves. This would increase speed in manufacturing and improve manufacturing repeatability.

References

[1] H. Zhu and W. J. Book, "Practical structure design and control for digital clay," vol. 73, American Society of Mechanical Engineers (ASME), 2004, pp. 1051–1058. DOI: 10.1115/IMECE2004-59743.

[2] R. Hashem, D. Browne, W. Xu, and M. Stommel, *Control of a Soft-Bodied XY Peristaltic Table for Delicate Sorting*. 2016, ISBN: 9781479984640.

[3] Z. Deng, M. Stommel, and W. Xu, "Mechatronics design, modeling, and characterization of a soft robotic table for object manipulation on surface," *IEEE/ASME Transactions on Mechatronics*, vol. 23, pp. 2715–2725, 6 Dec. 2018, ISSN: 10834435. DOI: 10.1109/TMECH.2018.2873259.

[4] P. Rothemund, A. Ainla, L. Belding, *et al.*, "A soft, bistable valve for autonomous control of soft actuators," 2018. [Online]. Available: http://robotics.sciencemag.org/.

[5] M. A. Robertson, M. Murakami, W. Felt, and J. Paik, "A compact modular soft surface with reconfigurable shape and stiffness," *IEEE/ASME Transactions on Mechatronics*, vol. 24, pp. 16–24, 1 Feb. 2019, ISSN: 10834435. DOI: 10.1109/TMECH.2018.2878621.

[6] N. W. Bartlett, K. P. Becker, and R. J. Wood, "A fluidic demultiplexer for controlling large arrays of soft actuators," *Soft Matter*, vol. 16, pp. 5871–5877, 25 Jul. 2020, ISSN: 17446848. DOI: 10.1039/c9sm02502b.

[7] K. P. Becker, Y. Chen, and R. J. Wood, "Mechanically programmable dip molding of high aspect ratio soft actuator arrays," *Advanced Functional Materials*, vol. 30, 12 Mar. 2020, ISSN: 16163028. DOI: 10.1002/adfm.201908919.

[8] Z. Deng, M. Stommel, and W. Xu, "Operation planning and closed-loop control of a soft robotic table for simultaneous multiple-object manipulation," *IEEE Transactions on Automation Science and Engineering*, vol. 17, pp. 981–990, 2 Apr. 2020, ISSN: 15583783. DOI: 10.1109/TASE.2019.2953292.

[9] J. K. Zou, M. K. Yang, and G. Q. Jin, "A five-way directional soft valve with a case study: A starfish like soft robot," Institute of Electrical and Electronics Engineers Inc., Sep. 2020, pp. 130–134, ISBN: 9781728198880. DOI: 10.1109/CACRE50138.2020.9230177.

[10] S. Hoangid, K. Karydisid, P. Brisk, and W. H. Groverid, "A pneumatic random-access memory for controlling soft robots," 2021. DOI: 10.1371/journal.pone.0254524. [Online]. Available: https://doi.org/10.1371/journal.pone.0254524.

[11] M. S. Xavier, A. J. Fleming, and Y. K. Yong, "Finite element modeling of soft fluidic actuators: Overview and recent developments," *Advanced Intelligent Systems*, vol. 3, p. 2 000 187, 2 Feb. 2021, ISSN: 2640-4567. DOI: 10.1002/aisy.202000187.

[12] "Measurement of fluid flow by means of pressure differential devices inserted in circular cross-section conduits running full — part 1: General principles and requirements," International Organization for Standardization, Geneva, CH, Standard, 2020.

A Literature review

Delft University of Technology

Litrature review soft compliant surface

Authors:
Koen Guurink (5181615)

December 21, 2022

Abstract

Soft actuated surfaces can reconfigure their shape and are made of silicone or other soft materials. Due to the innate softness delicate objects such as food or wafers can be handeld with out the risk of damage. In the medical domain such surfaces/devices could be used for supporting hollow organs. Other examples include computer-human interaction and transportation. The objective of this paper is to review the state-of-the-art and advances of rigid and soft actuated surfaces and the methods to activate and control them. It covers the aspects of actuation units, connecting them to a surface, elements for activating them through hydraulic or electromagnetic means and manufacturing methods. This paper highlights 3 key gaps in the literature: passive control, ridged base and sensing. Passive control is defined as having more outputs than inputs. This is needed to increase the area and the resolution of a surface. Most actuated surfaces have a ridged base, a flexible base could have applications in the biomedical field. The displacement of a soft actuated surface is measured using a vision camera. This significantly increases the required room needed for an actuated surface.

1 Introduction

Soft robotics is a newly emerging field with many potential applications. Soft robotics are robots made of silicone or other soft materials, due to the innate softness delicate materials can easily be handled, this is due to compliance matching.

An example for biomedical applications is the use of a heart assist device. The reason soft robotics is well suited for this application is the high innate compliance, damaging soft materials is not possible due to compliance matching. Therefore it can be interesting to create a soft robotic surface. There is not a lot of research done in this particular area of soft robotics. A soft actuated surface could have applications in transporting delicate materials or for creating better technology for assisting organs in the biomedical field.

The goal of this paper is to review the state-of-the-art and advances of rigid and soft actuated surfaces and the methods to activate and control them. The fallowing topics will be covered: ridged actuated surfaces, soft actuated surfaces, control architecture, soft pads, valves and manufacturing techniques, finally a conclusion will be made made about the general gaps in the literature. This paper will consider rigid actuators, a focus would be put on: the control architecture, achieved forces, bandwidth and stroke. The reason for this is that rigid actuators had more time to develop, so it is possible to borrow some concepts from that field. For soft surface actuators the same details would be considered as rigid surfaces. Actuated surfaces have lots of inputs and outputs, it is investigated what was done in soft robotic to reduce the number of inputs and thus minimize the complexity of controlling a surface. A distinction is made between soft robotic pads and soft robotic surfaces, the reason for this is that those 2 concepts operate a different way. For controlling a surface valves are needed, these valves also need to be compliant to fully use the properties of soft robotics. That is why soft-compliant valves are relevant for this paper. An actuated surface will most likely have complex channels and shapes, for that reason brief consideration will be made in manufacturing techniques.

A summary of the technical performance can be found in Figure 1. A note why Mosadegh *et al* has a high resolution and bandwidth is they use piezoelectric bimorph actuators.

Reference	Resolution (mm^2/actuator)	Area (mm^2)	Bandwith (hz)	Max force (N)	Stroke (mm)
Nakagaki et al	392	100x200	ng	3,6	120
Siu et al	55	90x175	ng	ng	50
haptx et al	aprox 50	aprox 30x20	aprox 4	ng	2
Stoll et al	2704	936x624	ng	ng	10-20
Salerno et al	10000	500x500	20	x	30
Zhu et al	100	100x100	aprox 10	ng	60
Hashem et al	3600	300x300	ng	ng	30
Robertson et al	639	93x110	ng	5	10
Raeisinezhad et al	aprox 2328	X	ng	aprox 2	31,5
Deng et al	1296	160x160	ng	apox 2,5	aprox 9
mosadegh et al	aprox 105	76x86	40	0,18	0,7

Figure 1: X=not inplemated,ng=not given

2 Rigid actuated surfaces

Soft robotics is a very new field. It can therefore be fruitful to consider rigid operated surfaces because this field had more time to develop and some concepts may be applicable on soft actuated surfaces. A focus in 2 areas has been made in human computer interaction and transporting surfaces. The reason for this is that these research areas make great use of the concept of an actuated surface. With each research project the achieved bandwidth, force and stroke and resolution will be highlighted if they are given. The reason for this is that these are important parameters of a actuated surface. It will also be highlighted how the setup is constructed (actuators,valves,ect), this is done to get insight what techniques are commonly used in actuated surfaces.

2.1 Human-machine interaction

The field of human-machine interaction has used the concept of actuated surfaces that can be used to generate a shape for a tactile experience.

Nakagaki *et al.* [26] studied the haptic connection between human and machine. To do this they build a actuated surface which they called inForce, the design can be seen in Figure 2. They implemented a PID controller with a linear actuators. With this control loop stiffness can be mimicked. The actuators had integrated hall sensors used for measuring displacement. To detect the exerted force the drawn current is measured and converted

to a force. The resolution of each pin was 19.8 mm^2, resolution is defined as the total area divided by the number of actuators. The accuracy of the force is 0.4 N, the precision for this displacement is 120μm. What can be noted is that the entire set has a large length 120 cm, see Figure 3. The rest of their research and results mainly focus on human-computer interaction, what is more relevant for this paper is the technical aspect of their surface.

Figure 2: inForce system

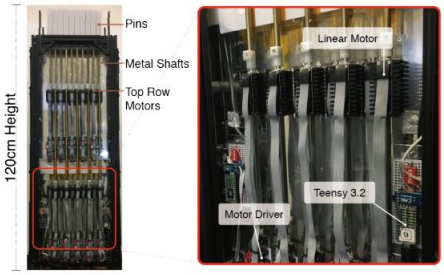

Figure 3: inForce side view [26]

Siu *et al* [23] designed a surface similar to Nagasaki *et al.*. A key difference with Nakagaki *et al.* is that this design has a higher number of pins (288 pins) and the actuated surface is smaller (9 x 17.5 cm). Siu *et al* call their design ShapeShift, see Figure 4. Their study aimed to increase the operating area of a surface without having a physically larger surface. The way they achieved this was putting system on wheels that rolls to the desired area. The reason for this is that the system can then simulate a larger area in a VR environment by just rolling to the designated location. This is done to reduce the overall cost of these kind of pin systems. The pins are coupled by a nut and driven by a screw via a DC motor, at the end of the screw an extension is made to measure tick marks. These marks are integrated to gain the position. For the displacement they use a PID control scheme. Force feedback is not implemented in this design. This is the setup used to investigate human computer interaction. This work show how a a small surface could be leveraged to function as a larger surface in a VR environment.

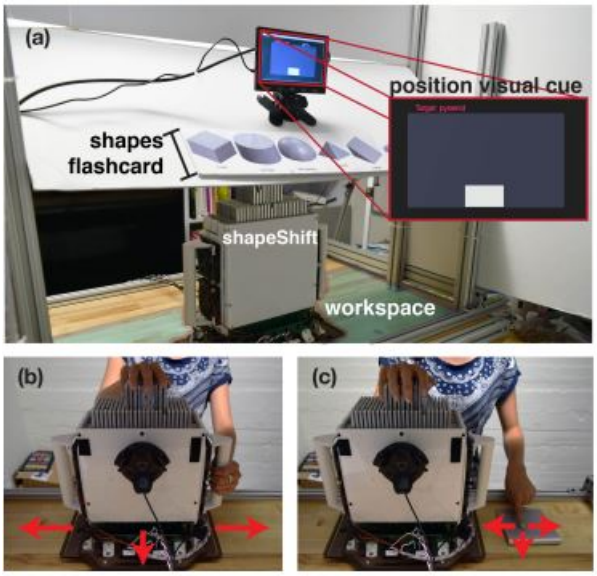

Figure 4: ShapeShift [23]

A practical example of an actuated surface is this VR-glove (Virtual reality) developed by the company HaptX [45]. The goal of this glove is to simulate tactile feelings in a VR environment. This is achieved by inflating a pneumatic actuators located at the palm and fingertips of the glove, the actuators on a fingertip can be seen in Figure 5. Unfortunately no research has been released. However the company has done some interviews online discussing some technical aspects [19]. No exact bandwidth was given but it in the interview it was claimed that it was in the ms range. Later it was mentioned that to convince a human brain of tactile feedback a bandwidth in the order of 250 ms must be achieved. The stroke of an actuator is around 2 mm.

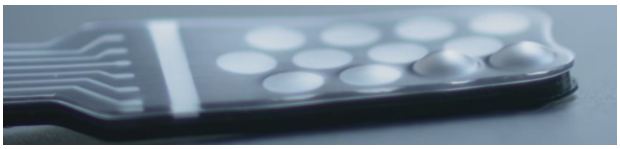

Figure 5: haptic unit,out of the glove[19]

2.2 Transporting surfaces

A other application of a actuated surface is transporting delicate objects. One of the earlier examples of a transporting surface was implemented by FESTO in 2013 [4]. FESTO made a surface to mimic waves to move the object around as seen in Figure 6. This was meant as an alternative for a standard conveyor belt. The system consists

of interconnected actuators that pushes an elastic surface up and down to mimic waves, the entire setup has 216 actuators with a stroke of 1-2 cm and has a area of 93.6 x 62.4 cm. Each valve has its own integrated valve and PCB, so everything can be controlled locally. This results in a plug-and-play type of control. To monitor the entire set up a vision camera was placed above of the surface. Unfortunately no research was released.

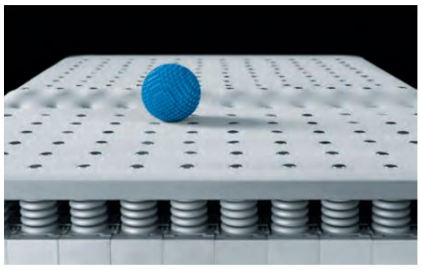

Figure 6: FESTO wave handeling[4]

Inspired by the work of FESTO Hashem *et al* [10] wanted to combine a soft surface with a riged actuation. As actuation they used NEMA17 stepper motors, as seen in Figure 7. This would produce a peristaltic moving table. Such a table was hypothesized to be useful for moving dedicated objects such as food. Their main way of measuring was with a vision camera. They trained a neural network to determine what the best way is to deform their surface. Their practical control system was a master-slave system, in other words, the master send commands and the slaves execute them. In the paper they implemented an open loop sinus generation and closed loop pathfinding algorithm control schemes. Their entire setup consist of a grid of 5x5 actuators the area was 300x300 mm. Movement in the x-y direction worked well, however the authors had difficulties creating waves under an angle in the x and y directions. The researchers hypothesized that this is caused by the training set of their neural network.

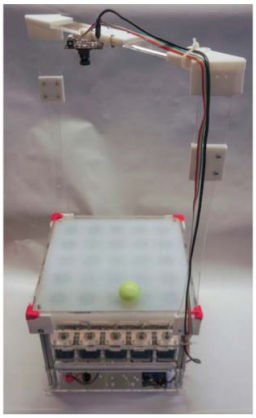

Figure 7: Peri-staltic Table[10]

Salerno *et al* [39] has created a design called the Oripixel Figure 8 that can extend, pitch and roll. This differs form most surfaces that can only extend. The pixel consists of an endeavored where 3 origami folded leg were connected. Each leg is powered by a servo motor, to control the motors each pixel has its own PCB board. The board of the pixel is then controlled by a master board. They implemented this desin in a 5x5 grid with a total size of 500x500 mm. The max z height is 35 mm and can roll and pitch 50 deg. As control scheme they used a PID controller. They implemented their master-slave command systems to send command to each servo motor. Salerno *et al* is one of the few reports focusing on pitch and roll.

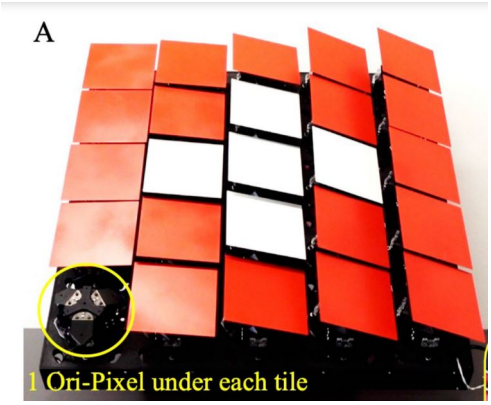

Figure 8: Oripixel[39]

The companies Cikoni [17] and Adapa [32] provide a shape changing rigid surface used for composite molding. The Dynapixele made by Cikoni by can be seen in Figure 9. Unfortunately no scientific literature can be found on these products, but it demonstrates that a large stroke and high stiffness can be achieved.

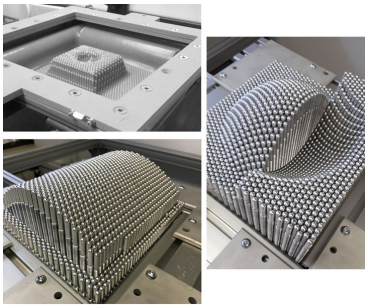

Figure 9: Dynapixele by Cikoni[17]

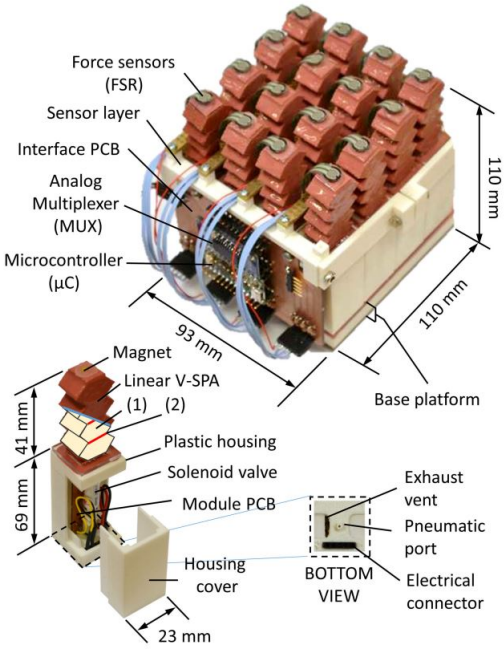

Figure 10: Vacuum powered soft array[29]

3 Soft robotic surface

In this section a closer look will be given to soft robotic surfaces. Actuated surfaces can be defined as a array of actuators.

https://www.overleaf.com/project/61938f99a2079766a840a97b
Robertson *et al* [29] have designed a haptic and re-configurable surface that is highly modular. The reason for this is the researchers wanted to extend the utility of a shape changing surface, for an overview see Figure 10. They made a 4x4 array of vacuum powered actuators. The size of the entire setup is 93 x 110 x 11 mm. Each actuator has its own solenoid valve and PCB. On the top of each actuator there is a force sensor, for an overview see Figure 10. Each actuator can be controlled locally, this means the researchers went for a plug-and-play approach. It is thus possible to rearrange the setup with these actuators and they would still be controllable. The height of the actuator is estimated based on the negative pressure it receives. The actuator has a length of 4 cm and a max free contraction of 1 cm. A force sensor is mounted on the tip of the actuator. The wires of the sensor were routed to the sides of actuators. Note that these sensors were used only in experiments were the mimicked stiffens. With this sensor a feedback control system is implemented. The max force an actuator could provide is 5 N. In the paper the researchers demonstrated a several properties. They demonstrated object manipulation with different objects each varying in size and shape. In other experiments, they could mimic passive stiffness.

Another example where a force sensor is integrated into the tip is in the work of Raeisinezhad *et al* [38]. In the paper the researchers discuss their soft robotic actuator, this actuator will be connected into a grid in a later stadium. Raeisinezhad *et al* call their design IntelliPad, a cross-section can be seen in Figure 11. The surface was developed to combat bed/sitting sores that come when a patient sits or lays down for a long time, the main cause of this injury is shear stress. The goal of having an actuated surface is to reduce the stresses on the skin of the patient. The actuators consist of different chambers that can expand or put into vacuum to created displacement into the X-Y-Z direction. On the tip of each actuator there is a sensor that measures the force in the normal direction, from the normal force the shear stress can be estimated. A full grid was not realized but test were conducted using 3 actuators each with their own valve. In the test with 3 actuators in a row the researchers redistributed the normal force. The reason this literature is relevant is that it is one of the few examples where a soft actuated surface also must provide movement in the x and y direction.

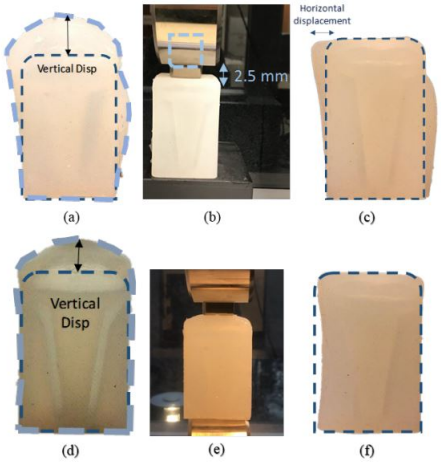

Figure 11: IntelliPad[38]

Deng *et al* have design a soft table [18] that can transport delicate objects like food, silicon wafers, etc, the setup can be seen in Figure 13. For movement the researchers looked at nature and tried to mimic the movement of a Caterpillar, this can be seen in Figure 12. By inflating and deflating chambers in a certain order movement on an object is achieved. The design of the actuators was most focused on the X-Y movement. In a continuation of this project Deng *et al* [35] tried to improve their table. The first attempt was with a open loop control system, they changed it to a closed loop. This is a feedback loop that works with a vision camera as the sensor. The end goal of this project is to created a table that can move delicate objects such as wafers and food. To control their surface the researcher compared a PI and a back stepping control systems, the PI system performed better. The X and Y errors were 3.8 and 4 mm. The angle error was 12.8 deg. The total surface is around 160x160 mm^2 based on the pictures.

Bailey *et al* [9] looked at sensing for a soft robotic table. Controlling was done with an open loop control system. To measure the deflection of their actuator an infra red sensor was placed inside the actuator, as seen in Figure 14. The researchers experimented with 2 different opaque membranes, the opaqueness had some effect on the performance, more research is needed to optimize it. The measurement range was between 15 and 25 mm. The results showed that there was little disturbance in measuring, with proper filtering the researchers claim it could work in the sub mm range.

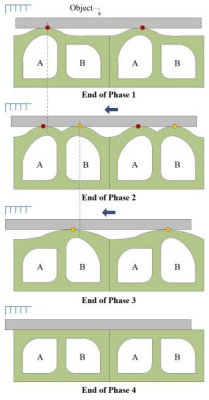

Figure 12: Movement of table [18]

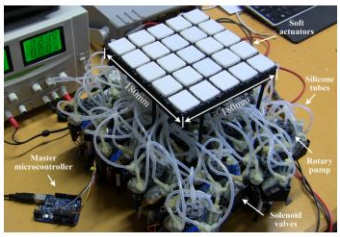

Figure 13: Soft table [18]

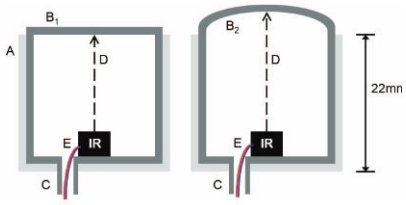

Figure 14: Schematic sensing[9]

Mosadegh *et al* [6] developed a changing Braille interface. Commercially available displays are available but are quite expensive. A single line display could cost around 1000 euro [50]. The reason for this is a ridged braille display uses piezoelectric bimorph actuators for a single dot. They controlled a grid (64 pins) with 2 valves per unit these are inflow and outflow powered by a piezo-electric actuator. What was interesting is that all these valves were soft, the pins were not. These valves are controlled with a master system directly underneath it as seen in Figure 15. The master valves are piezo electric. The entire setup was controlled with the use of a controller and a flow sensor.

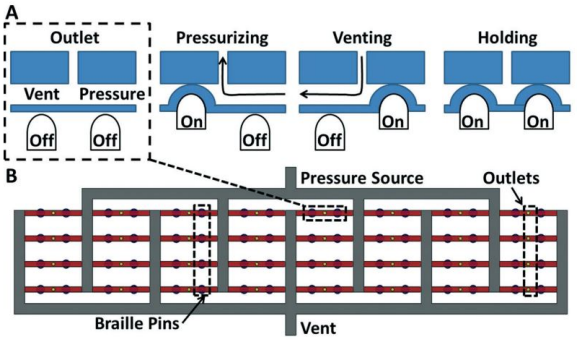

Figure 15: Schematic braile display [6]

Stanley *et al* [12] aims to design a surface that mimics skin stiffness. When mimicking stiffness in a surface it only works in the direction of the actuator, The stiffness in the shear direction is not captured, an application of having this kind of surface could be in training medical professionals. Stanley *et al* aims to capture this by having a surface with with variable stiffness. This is done by putting granular material(grounded coffee) under a variable vacuum. This work is an improvement of their previous work [3], [8]. The surface consists of a grid of 3x4 cells, as seen in Figure 16. When the surface is depressurized a wire located under the surface that is connected to a torsional spring reels in the surface back into position, the torsional spring is connected to a reel that can be fixed in position by a solenoid. For the control loop a closed-loop PID controller is used. To measure the height a Kinect (vison camera) is used. To estimate the needed pressure the researchers created an algorithm to calculate the required inputs. Stanley *et al* did not measure the performance of their entire surface but did some tests on a single cell. The researchers specifically measured the spring stiffness and damping constant of 1 cell. The average error of all their tests was $2.87x10^{-4}m$ and 1.41 N. The researchers claim that with a higher resolution their algorithm could better capture the shape of the provided inputs.

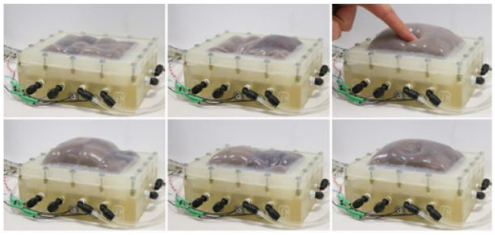

Figure 16: pneumatic jamming [12]

4 control architecture

In the research mentioned earlier the general setup of the physical hardware(valves, actuators,etc) is the mostly same, meaning that each actuator has its own valve and or motor. The problem with this is that controlling a large number of actuators would be a challenge, this is due to the scaling problem. The terms scaling problems means that the actuators required for a square surface goes up exponentially. In the following papers a solution has been implemented to solve this problem.

Zhu *et al* [2] was one of the earliest to consider controlling a actuated surface. The researchers created a pin array of 10x10 cells that has an area of 100x100 mm in area, as seen in Figure 18. The purpose of their research was to create a surface that functions as a computer input and output interface. In the paper Zhu *et al* explore different kinds of methods of sensing the height, They first tried to measure the height of the actuator with the use of direct change in capacitance, but this was dropped due to noise. For sensing the researchers settled on a sliding ring over a plate that has an AC voltage put onto it, with that the change in capacitance can be better detected. To measure the force a pressure sensor was integrated into each valve. For controlling their interface they used a novel kind of controlling scheme. They did not use the standard master-slave system. Their passive control system was an adapted scheme used primarily in led arrays, see Figure 17. This means the way the systems scaled is for n^2 arrays can be driven by 2n valves. Each actuator has a 1/2 valve with a hydraulic input for control. If the vertical row is pressurized the valve is open, then the horizontal row needs to be pressurized to get flow through the valve into the actuator.

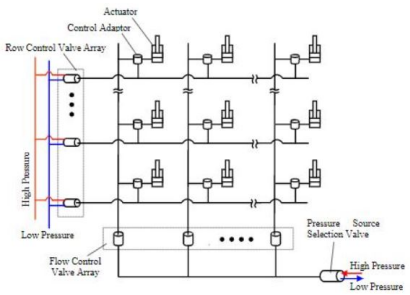

Figure 17: Digital clay [2]

Bartlett *et al* [33] Designed a demultiplexer that

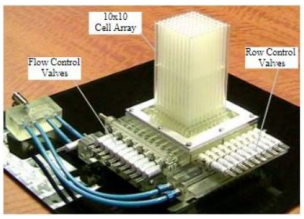

Figure 18: Digital clay [2]

can power soft actuators. In the paper a microfluidics system is used to control soft bending actuators with 3 DOF (degree of freedom). The microfluid channels are made in a piece of acrylic sheet as seen in Figure 19. The valves used to close the channels are quake valves. The entire control scheme is a multiplexer, This means it can control 8 outputs with only 3 inputs. In theory this control scheme could scale with n inputs for 2^n outputs. No information was given of the maximum achievable bandwidth.

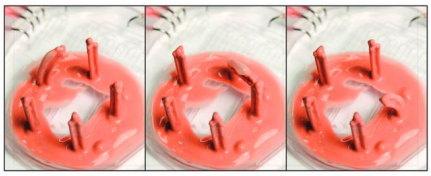

Figure 19: Bending array with demultiplexer [33]

Hoangid *et al* [46] design a pneumatically operated RAM (random access memory) chip that can control 8 fingers with only 3 inputs. The chip is made of 2 acrylic plates with an elastomer in between, a close up can be seen on Figure 20. With this chip they control 8 vacuum powered fingers with the use of 3 solenoids. With the use of the chip each finger can be set and reset, the chip uses a vacuum as a form of memory. Setting is bending the finger. When a finger is set it will retain its shape but due to leakage the finger will return to its original position, in an hour a finger will lose 10 % of its contraction. To demonstrate that the chip works it was programmed to play (slowly) a simple song on a piano, as seen in Figure 21. In the paper the researchers claim that they can control 2^{n-1} actuators with n valves.

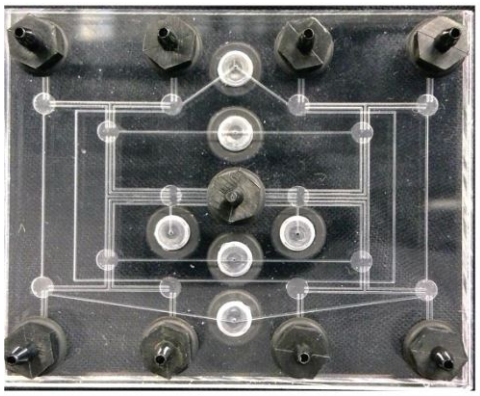

Figure 20: RAM chip [46]

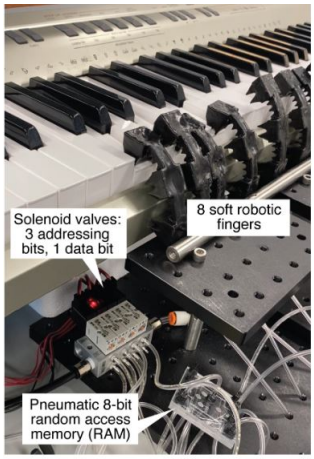

Figure 21: Fingers and chip [46]

5 Soft pads

This section describes a selection of soft robotic pads. A pad deforms in a continuous manner and linear surfaces consist of a grid of linear actuators. The other key distinction is that a surface need more inputs to function than a soft pad.

Chen *et al* [16] wanted to explore the possibilities of soft robotic sheets. In the paper the researchers built an analytical model with the use of virtual work and minimum potential energy, after that a prototype is made as seen in Figure 22. It consists of 2 bending actuators. Those actuators were 2 cylindrical bodies wrapped in nylon fiber, the air chamber was off-center, so when the body inflates it will bend. The rest of the surface was cast in Ecoflex-00-50. They later compared the analytic model with data from their prototype. The error of the model was 5 % of the length of the edge.

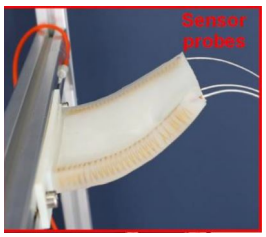

Figure 22: Bending pad[16]

Siefert *et al* [30] designed a pad that can change in multiple directions, as seen in Figure 23. The design is based on Acetabularia acetabulum, that is a plant that grows underwater and has a circular shape. The pad has multiple channels that can be inflated by a needle with no advance control, by varying the numbers and size of the channels Siefert *et al* can create different complex shapes. The researchers made multiple surfaces that change in different ways. The researchers created a program were the needed channels are calculated for a desired shape. The researchers used this for example to generate a face, the face matched roughly what was given. The predictions of the more simple pad matched there predictions better. Fabrication is achieved by using an open mold with the negatives of the channels, for the next step the open silicon is placed/dip on a sheet of uncured silicon to close of the top.

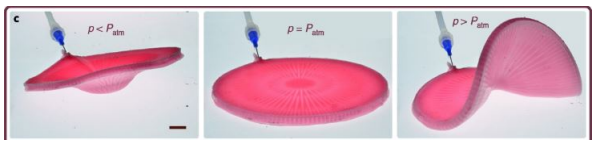

Figure 23: Shape-morphing elastomers [30]

Sun *et al* [41] continued their previous research [15], [31], [42]. They claim that most research in soft robotics goes into 1 degree of freedom(DOF) actuation unit, for this reason the researchers wanted to explore a more 2D shape. A analytical model is created that captures the relation between bending and pressure, after this a prototype is created. The pad is manufactured out of silicon and heavily reinforced with fibers and can generate a blocked force up to 70N. With the prototype testing has been done to validate the results. The blocked force relation of the pad deviates at 60 kPa, before that point the results are matching with a overall standard deviation of 3N. As an example for an practical application the researchers used the Pad to support a human arm.

Lu *et al* [14] have designed a soft robotic tongue. This tongue could be used to conduct (medical) research on. The tongue itself has 6 chambers for pressurizing, the tongue can be seen in Figure 24. The top and bottom were made of Ecolfex 030 silicon in those parts the actuators were molded in, the middle layer is made from PDMS. Each actuator inside the tongue had its own control valve for infill and outflow and pressure sensor. To measure the displacement of the tongue they used a motion tracking system, trackers were placed on the tongue. They made the tongue take different shapes (roll-up,roll-down, Elongation, ect). There FEM results matched the experimental results with an avarage error of 11,36%. The same test were done again to test to reputability, there probability density function most peakes were around 0.025 mm, but the result varied depending on the type of movement the tongue made.

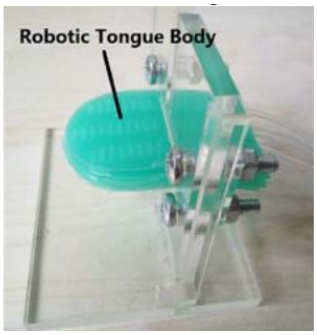

Figure 24: Soft Tongue[14]

Liu *et al* [48] created a surface using liquid crystal elastomers (LCE) that has the ability to reprogram its deformation, this is different form other pads that can only deform in 1 predefined way. There are 2 liquid crystal elastomers (LCE) grids on top of each other, as seem in Figure 25. A grid consists of wires going vertical or horizontal, those wires are not interconnected. To space out the grids sheet of Kapton tape is used in a wave-like structure to separate the 2 grids. By putting current through the coils the surface morphs in different configurations. The time it takes to complete a deformation is around 2 minutes. The surface could also support a load of 200 grams. The researchers claim that their design is also scale free in the micro and macro direction. A suggested improvement by the researchers was implementing a

feedback system.

Figure 25: LCE grid[48]

6 Valve's

Controlling a soft robot requires valves. It can be preferably these valves are also soft, this is the case when the entire robot needs to be compliant. In this section a look is made with ridged and soft on/off valve and soft check valves.

6.1 Ridged On/off valves

To better understand the difference in performance between a ridged and soft valve a look is made on rigid valves. Rigid valves are used in soft robotics, however these valves do not possess the inherent compliance that soft valves have.
In the review paper of McDonald *et al* [49] they review a couple of soft valves and rigid valves. They compare the bandwidth, max pressures, and other points relevant for soft robotics. In general rigid valves have higher bandwidth and higher max pressure than soft valves. Rigid valves can achieve a bandwidth between 10 and 200 hertz and a max pressure between 34 689 kPa.

6.2 Soft on/off valves

A trend in soft robotics is using micro fluidics, a example can be found is in the work of Ranzani *et al* [21] who created a soft robot using microfluidics. A valve that is used extensively in microfluidics is the quake valve. This valve consists of 2 lines on top of each other with a membrane in between. When the control line is pressurized the source line is restricted in flow, this reduces or completely blocks the flow of the fluid. A schematic can be found in Figure 26.

Using this type of valve Zou *et al* [43] created a soft robot with this valve as seen in Figure 27.

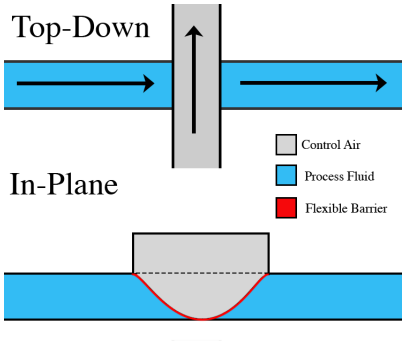

Figure 26: Quake valve[20]

The Researchers used water-soluble 3D printed PVA (Polyvinyl Alcohol) as a lost core method for casting the silicone. An overview of this method can be seen in Figure 28. This type of valve is used to create a soft robot in the shape of a starfish. This design has been implemented 5 times in the center of the starfish. The design has a high fatigue rate, the holding pressure has dropped after 50 cycles. The max holding pressure was 60 kPa with a membrane thickness of 2,5 mm.

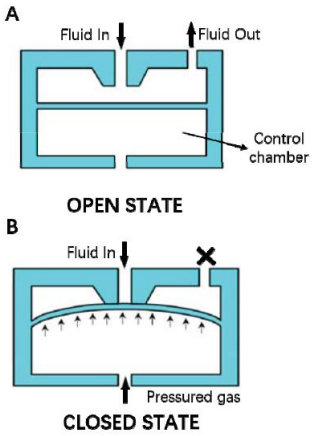

Figure 27: Soft quake valve[43]

Luo *et al* [25] looked with a analytical approach at an kink valve. A kink valve is an elastomer tube that kinks when compressed. When a tube is kinked the pressure flow is completely cut off, as seen in Figure 29. A undesired effect is that sometimes the tube will twist instead of buckling, a twisted valve will still allow flow and thus will not function properly as a valve. In the paper a FEM model is made and the results are compared experimental results the results matched with the FEM analysis.

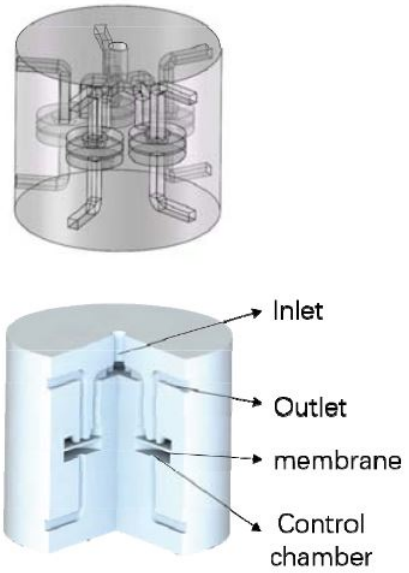

Figure 28: Core of starfish soft robot[43]

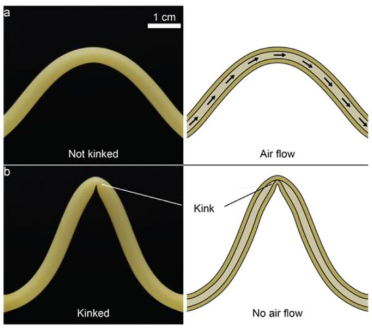

Figure 29: Buckle valve[25]

Rothemund *et al* [22] designed a more developed version of the kink valve by creating a 3/2 valve. It is a bi-stable valve that does not need continuous pressurizing, a schematic overview can be found in Figure 30. When inflating a chamber the membrane will flip in the direction where the pressure is less in that state it will block the other tube. The valve has a diameter of around 4 cm and is 4 cm tall. This valve was also used to make a completely soft robot, as done by Drotman *et al* [44]. This robot has an oscillatory system that is used to control the timing when the legs move. This oscillatory system is explored more Preston *et al* [27]. In a later study this design has been used to make logic gates (AND, OR, etc) these gates are again researched more by Preston *et al* [28].

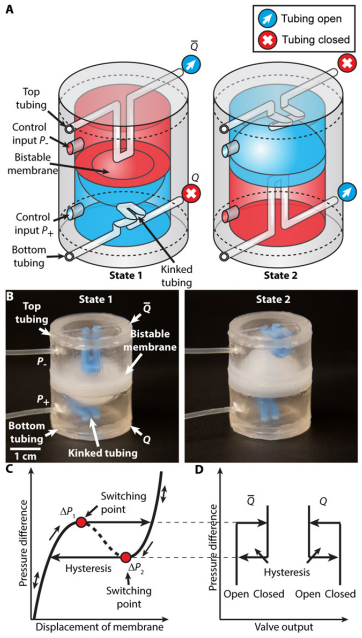

Figure 30: Bi-stable valve[22]

Miyaki *et al* [37] designed a oscillatory system that produced a wave-like signal with a constant pressure supply, the way it functions can be seen in Figure 31. When the airbag is pressurized it moves the magnet close to the other magnet and snaps into position, this will close the other line. To reset the system the bag of another valve has to be pressurized (not shown on the diagram). On this bag there is a magnet attached that resets the first magnet. To create a wave pattern the valves are connected in such a way that they constantly set and reset each other, see Figure 32.

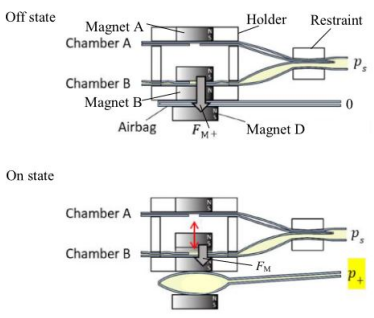

Figure 31: Schematic magnetic soft valve[37]

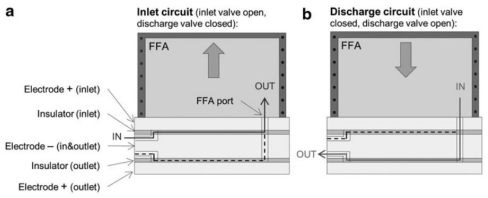

Figure 33: Electrorheological Valve[13]

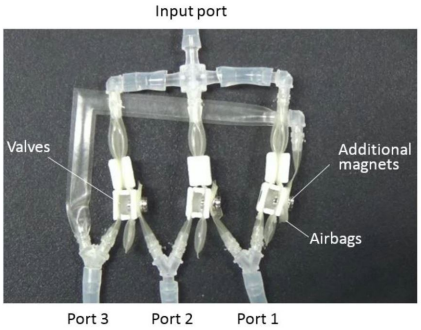

Figure 32: Magnetic soft valve[37]

The valves mentioned until now operate on pneumatic or hydraulics fluids, it can be noted that smart fluids also provide a solution. In the next section, a closer look will be made at smart fluid valves.

Tonazzini *et al* [13] created a valve for rlectrorheological fluid. This kind of fluid will increase its apparent viscosity in the order of 10000 when subjected to an electric field of around around 5 kV. The time it takes to change viscosity is in the order of ms. The valve that the researchers created can stand up to a pressure of 1 MPa. With 2 of these vales stacked on top of each other the researchers can control the in and outflow of an FFA (flexible fluidic actuator) as seen in Figure 33.

Another example is done by Mcdonald *et al* [36] they designed a valve using MR-fluid. Magnetorheological fluid (MR) is a fluid with small micron size ferrous particles, when this fluid is subjected to a magnetic field the particles align and increase the yield strength of the fluid. With this property valves can be made to operate a soft robot, in Figure 34 this can be seen in action. The researchers used permanents magnets but also electromagnets. A disadvantage of an electromagnet is that the temperature will increase, with the used coil it took 200 seconds to reach 100 degrees. The max pressure that the valve could handle was around 3.5 kPa with a flow of 25 mL/s. The switching time of the valve was around 0.4 seconds.

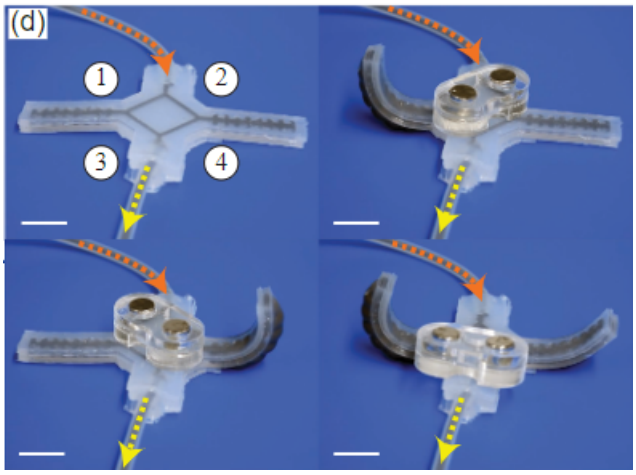

Figure 34: MR-valve[36]

6.3 Check valves

To control the flow of a fluid check valves are needed to stop back flow and to maintain pressure.
An example of a compliant check valve in the industry is the "Duckbill valve" as seen in Figure 35. They are small in size, the smallest one found had a diameter of 2 mm [51]. Advantages are that they are low maintenance, cost-effective, and have low opening pressure. Unfortunately, no data sheets have been found for duckbill valves for small sizes. One of the few papers [1] that could be found describes an analytical derivation of the pressure drop of such valve.

Another commonly used soft valve is the cross

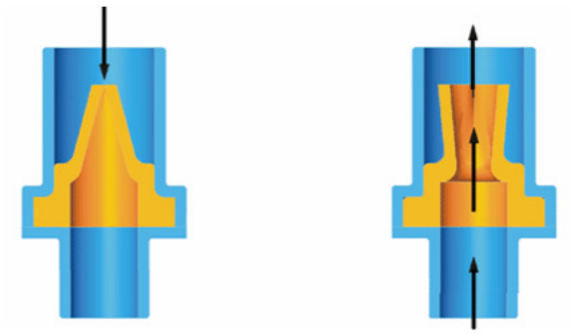

Figure 35: Duckbill[51]

slit valve. An example in everyday use is in the cap of a lotion, see Figure 36

Figure 36: Cross slit [11]

Jin *et al* [47] have designed 4 different kinds of mechanical valves that can be integrated into soft robotics, see Figure 37. A and B are viscus flow valves that are constructed with an acrylic plate and small tube, these valves create a transient pressure difference around 10 kPa by limiting the flow due to the narrow cross section, the difference between the two valves is that B has an extra check valve. In C you can see the hysteresis valve and bistable valve. Design wise they look the same, The difference is the thickness of the membrane. There is a piston where the input pressure is pushing against, When the input pressure is around 20 kPa the metal plate connected to the piston will snap in a new configuration were there is a is a notch that allows for air to pass. With the use of these valves, the researchers made a rolling robot and a robot that climbs up a tube powered by a single supply line were all movements were repeated.

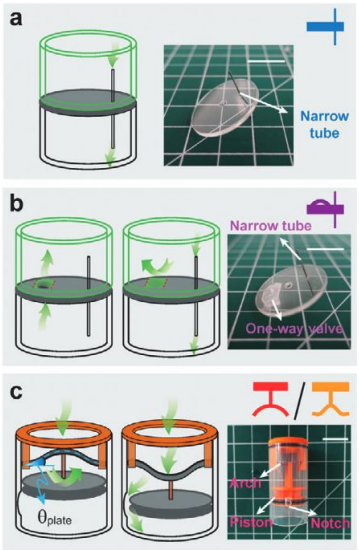

Figure 37: 4 Mechanical valves [47]

7 Manufacturing techniques

The shape and function of soft robotics are dependent on the manufacturing techniques, therefore it can be fruitful to look at different techniques. The technique's covered are ink jet printing, lost core in silicone, zero volume and open casting bending actuators.

Schlatter *et al* [40] designed a new type of actuator using ink jet printing. The actuator is power by dielectric elastomer actuators (DEAs) were the movement is a "zipping" kind of motion were relatively large fluids can be displaced. The researchers made a peristaltic pump and a surface that they call a "slug drive" due to having similar movement of a slug, the slug drive can be seen in Figure 38. With the slug drive an object for 0.26 g was moved with a speed of 3.6 μm s^{-1}.

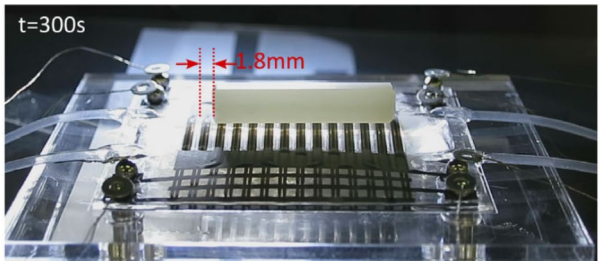

Figure 38: Slug drive[40]

Koivikko *et al* [24] explored the lost core method in silicone molding using different sacrificial materials. The focus was: HIPS(High Impact Polystyrene), PVA (Poly-Vinyl-Alcohol), PVB (Polyvinyl butyral), and ABS(Acrylonitrile Butadiene Styrene). They 3D printed a mold and used the materials mentioned earlier as a sacrificial insert, later the mold is filled with silicone. To shorten the time it takes for the sacrifice material to dissolve the researchers looked at putting the material in an ultrasonic bath washer and magnetic stirrer. Their result was the time it takes to remove the sacrificial material. For example, PVA went from 24 hours to 6 hours with a magnetic stirrer, other materials also significantly reduced the time to dissolve. The test was repeated with a ultrasonic bath the result for pva was a dissolving time of 5 hours. Another conclusion was that HIPs were less suitable for a sacrificial layer, this was due to swelling and could crack the 3D printed mold.

Most actuated surfaces are a collection of single

actuators. The following 2 production techniques create more integrated units.

Park *et al* [7] have developed a soft robot to help infants train there legs. What is more relevant in their paper is their production technique of making actuators, they call it zero volume actuators, a schematic can be seen in Figure 39. Galloway(one of the researchers) [5] used this technique to make a grid of actuators as seen in Figure 40. A prototype is build and the actuators are tested on contraction, the force that was achieved was a maximum 38 N with a stoke of 18 mm

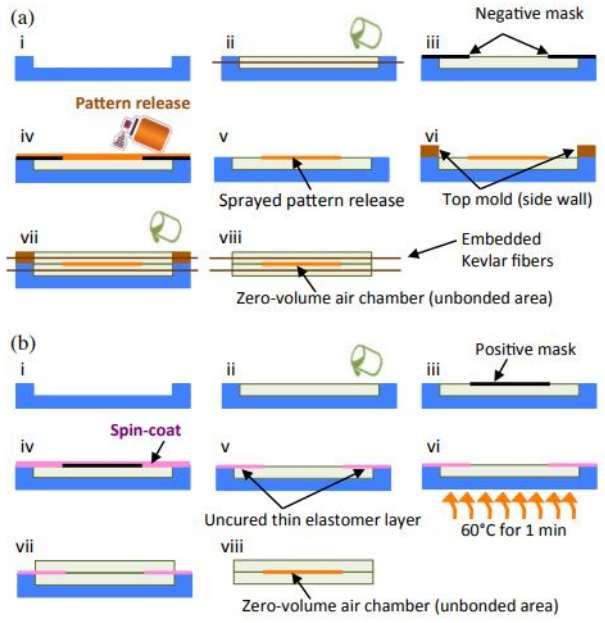

Figure 39: Zero volume actuator manufacturing[7]

Figure 40: Zero volume actuator [5]

Becker *et al* [34] explores a production technique that makes an array of bending actuators. The paper explores 4 different techniques. The techniques are:curing under an angle, putting a fiber on 1 side, curing under a electric potential,forcing surface tension by having a non cylindrical internal pin and curing under 90 degrees. With the use of these techniques one side of the actuator will become thicker and when put under pressure the actuator will bend in the thinner direction. The control of each actuator is dependent on the design of the surface, for example it can be seen that one row is actuated in the square actuator in Figure 41 each row can be activated but not each actuator individually. The outside diameter is determined by the number of silicon coats. The smallest bending actors that could be created had an internal diameter of 1.59 mm, it has to be noted that larger internal diameters have been used up to 6 mm. In the paper they also examined the pull force of an actuator. The pull force is also examined and is dependent on the way the actuator is manufactured, the forces measured were between 0.25 and 2 N for a single actuator.

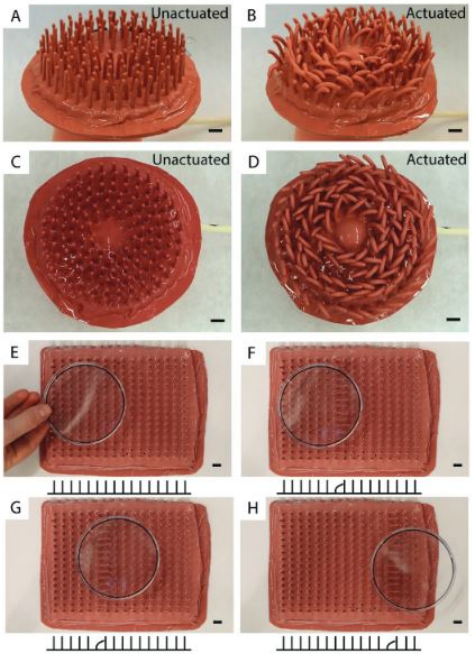

Figure 41: Bending array[34]

8 Discussions

This paper gives a overview of the state of the art of an actuated surface's. A consideration was made on rigid actuated surfaces, soft actuated surfaces and the different types of valves. The goal of this paper was to identify the knowledge gaps, these gaps will now be highlighted and discussed.

It can be noted that most linear actuated soft surfaces are not one integrated unit, meaning that single units of soft actuators are put into a grid.

A strength of soft robotics is that components can be integrated into a single unit, this can be explored further.

By giving each actuator its own control valve a actuated surface will suffer from a scaling problem. Solutions have to be found to reduce to number of inputs, otherwise high resolution or large area will not be possible. This problem is not fully explored in the field of soft actuated surfaces.

It is also noted that most actuated surfaces have a rigid base, meaning that they lack the compliance needed for a fully soft robot. Creating a soft surface with a complaint base could have applications in the biomedical field. Such a surface could be used to support a weakened heart.

Sensing is essential for controlling a actuated surface, but this has been extensively done force sensors have been used sparsely, but the main bottleneck is displacement. Most soft actuated surfaces measure this with the use of a vision camera, but this greatly limits the space required for operating a surface. Some designs try to get around this by estimating the displacement by measuring the pressure.

9 Conclusion

The aim of this paper was to give a overview of the state of the art of actuated surfaces and identify the knowledge gaps in the field.

One of the gasp is that a more integrated approach could provide more useful applications, in particular having a flexible base. This could have application in the biomedical field supporting hollow organs.

At the time of writing deflection is mostly measured using vision cameras or estimated based on the input. A more direct approach to measuring has to be developed to improve the accuracy.

More solutions have to be found to reduce the required number of inputs and still work for a large number of outputs. This is needed to improve the scalability of a soft actuated surface.

References

[1] J. H. Lee, D. L. Wilkinson, and I. R. Wood, "On the head-discharge relation of a duckbill elastomer check valve," *Journal of Hydraulic Research*, vol. 39, pp. 619–627, 6 2001, ISSN: 00221686. DOI: 10.1080/00221686.2001.9628291.

[2] H. Zhu and W. J. Book, "Practical structure design and control for digital clay," vol. 73, American Society of Mechanical Engineers (ASME), 2004, pp. 1051–1058. DOI: 10.1115/IMECE2004-59743.

[3] A. A. Stanley, J. C. Gwilliam, and A. M. Okamura, "Haptic jamming: A deformable geometry, variable stiffness tactile display using pneumatics and particle jamming," 2013.

[4] W. Stoll, E. Knubben, and A. Hildebrandt, "Wavehandling conveying and sorting in one," 2013.

[5] K. Galloway, *Zero volume air chambers, nerdlab*, 2014. [Online]. Available: http://www.kevincgalloway.com/portfolio/zero-volume-air-chambers/.

[6] B. Mosadegh, A. D. Mazzeo, R. F. Shepherd, *et al.*, "Control of soft machines using actuators operated by a braille display," *Lab on a Chip*, vol. 14, pp. 189–199, 1 Jan. 2014, ISSN: 14730189. DOI: 10.1039/c3lc51083b.

[7] Y.-L. Park, J. Santos, K. G. Galloway, E. C. Goldfield, and R. J. Wood, "A soft wearable robotic device for active knee motions using flatpneumatic artificial muscles," p. 6822, 2014.

[8] A. A. Stanley and A. M. Okamura, "Controllable surface haptics via particle jamming and pneumatics," *IEEE Transactions on Haptics*, vol. 8, pp. 20–30, 1 Jan. 2015, ISSN: 19391412. DOI: 10.1109/TOH.2015.2391093.

[9] D. G. (G. Bailey, G. S. Gupta, S. Marsland, *et al.*, *Proceedings of the 2016 International Conference of Image and Vision Computing New Zealand (IVCNZ)*. 2016, ISBN: 9781509027484.

[10] R. Hashem, D. Browne, W. Xu, and M. Stommel, *Control of a Soft-Bodied XY Peristaltic Table for Delicate Sorting*. 2016, ISBN: 9781479984640.

[11] s. gasket silicon, *Silicone one way valve from china manufacturer - silicongasket.com*, 2016. [Online]. Available: https://www.silicongasket.com/Silicone-One-Way-Valve-pd6855846.html.

[12] A. a Stanley, K. Hata, and A. Okamura, *2016 IEEE International Conference on Robotics and Automation : Stockholm, Sweden, May 16th 21st*. 2016, ISBN: 9781467380263.

[13] A. Tonazzini, A. Sadeghi, and B. Mazzolai, "Electrorheological valves for flexible fluidic actuators," *Soft Robotics*, vol. 3, pp. 34–41, 1 Mar. 2016, ISSN: 21695180. DOI: 10.1089/soro.2015.0015.

[14] X. Lu, W. Xu, and X. Li, "A soft robotic tongue-mechatronic design and surface reconstruction," *IEEE/ASME Transactions on Mechatronics*, vol. 22, pp. 2102–2110, 5 Oct. 2017, ISSN: 10834435. DOI: 10.1109/TMECH.2017.2748606.

[15] Y. Sun, J. Guo, T. M. Miller-Jackson, X. Liang, M. H. Ang, and R. C. H. Yeow, "Design and fabrication of a shape-morphing soft pneumatic actuator: Soft robotic pad," *IEEE International Conference on Intelligent Robots and Systems*, vol. 2017-September, 2017, ISSN: 21530866. DOI: 10.1109/IROS.2017.8206524.

[16] L. Chen, C. Yang, H. Wang, D. T. Branson, J. S. Dai, and R. Kang, "Design and modeling of a soft robotic surface with hyperelastic material," *Mechanism and Machine Theory*, vol. 130, 2018, ISSN: 0094114X. DOI: 10.1016/j.mechmachtheory.2018.08.010.

[17] cikoni, *Adaptive tooling technology for agile ramp;d and mass-customization of composite parts - cikoni - innovate. develop. realize. - composite engineering. carbon entwicklung - cfk (carbon)*, Nov. 2018. [Online]. Available: https://cikoni.com/en/adaptive-tooling-technology-for-mass-customization-of-composite-parts-and-fast-rd.

[18] Z. Deng, M. Stommel, and W. Xu, "Mechatronics design, modeling, and characterization of a soft robotic table for object manipulation on surface," *IEEE/ASME Transactions on Mechatronics*, vol. 23, pp. 2715–2725, 6 Dec. 2018, ISSN: 10834435. DOI: 10.1109/TMECH.2018.2873259.

[19] S. E. D. destinws2, *How do you make a virtual reality glove? - smarter every day 191*, Mar. 2018. [Online]. Available: https://www.youtube.com/watch?v=s-HAsxt9pV4.

[20] C. dude, *Quake_valve*, 2018.

[21] T. Ranzani, S. Russo, N. W. Bartlett, M. Wehner, and R. J. Wood, "Increasing the dimensionality of soft microstructures through injection-induced self-folding," *Advanced Materials*, vol. 30, 38 Sep. 2018, ISSN: 15214095. DOI: 10.1002/adma.201802739.

[22] P. Rothemund, A. Ainla, L. Belding, *et al.*, "A soft, bistable valve for autonomous control of soft actuators," 2018. [Online]. Available: http://robotics.sciencemag.org/.

[23] A. F. Siu, E. J. Gonzalez, S. Yuan, J. B. Ginsberg, and S. Follmer, "Shapeshift: 2d spatial manipulation and self-actuation of tabletop shape displays for tangible and haptic interaction," vol. 2018-April, Association for Computing Machinery, Apr. 2018, ISBN: 9781450356206. DOI: 10.1145/3173574.3173865.

[24] A. Koivikko and V. Sariola, *Fabrication of Soft Devices with Buried Fluid Channels by UsingSacrificial 3D Printed Molds*. 2019, ISBN: 9781538692608.

[25] K. Luo, P. Rothemund, G. M. Whitesides, and Z. Suo, "Soft kink valves," *Journal of the Mechanics and Physics of Solids*, vol. 131, pp. 230–239, Oct. 2019, ISSN: 00225096. DOI: 10.1016/j.jmps.2019.07.008.

[26] K. Nakagaki, D. Fitzgerald, Z. J. Ma, L. Vink, D. Levine, and H. Ishii, "Inforce: Bi-directional 'force' shape display for haptic interaction," Association for Computing Machinery, Inc, Mar. 2019, pp. 615–623, ISBN: 9781450361965. DOI: 10.1145/3294109.3295621.

[27] D. J. Preston, H. J. Jiang, V. Sanchez, *et al.*, "A soft ring oscillator," 2019. [Online]. Available: http://robotics.sciencemag.org/.

[28] D. J. Preston, P. Rothemund, H. J. Jiang, *et al.*, "Digital logic for soft devices," 2019. DOI: 10.1073/pnas.1820672116. [Online]. Available: www.pnas.org/cgi/doi/10.1073/pnas.1820672116.

[29] M. A. Robertson, M. Murakami, W. Felt, and J. Paik, "A compact modular soft surface with reconfigurable shape and stiffness," *IEEE/ASME Transactions on Mechatronics*, vol. 24, pp. 16–24, 1 Feb. 2019, ISSN: 10834435. DOI: 10.1109/TMECH.2018.2878621.

[30] E. Siefert, E. Reyssat, J. Bico, and B. Roman, "Bio-inspired pneumatic shape-morphing elastomers," 2019.

[31] Y. Sun, A. J. Y. Goh, M. Li, *et al.*, "Improved fabrication of soft robotic pad for wearable assistive devices," *Biosystems and Biorobotics*, vol. 22, 2019, ISSN: 21953570. DOI: 10.1007/978-3-030-01887-0_77.

[32] adapa, *Adaptive mould technical data comparison - adapa - adaptive moulds*, Oct. 2020. [Online]. Available: https://adapamoulds.com/adaptive-moulds-technical-data/.

[33] N. W. Bartlett, K. P. Becker, and R. J. Wood, "A fluidic demultiplexer for controlling large arrays of soft actuators," *Soft Matter*, vol. 16, pp. 5871–5877, 25 Jul. 2020, ISSN: 17446848. DOI: 10.1039/c9sm02502b.

[34] K. P. Becker, Y. Chen, and R. J. Wood, "Mechanically programmable dip molding of high aspect ratio soft actuator arrays," *Advanced Functional Materials*, vol. 30, 12 Mar. 2020, ISSN: 16163028. DOI: 10.1002/adfm.201908919.

[35] Z. Deng, M. Stommel, and W. Xu, "Operation planning and closed-loop control of a soft robotic table for simultaneous multiple-object manipulation," *IEEE Transactions on Automation Science and Engineering*, vol. 17, pp. 981–990, 2 Apr. 2020, ISSN: 15583783. DOI: 10.1109/TASE.2019.2953292.

[36] K. Mcdonald, A. Rendos, S. Woodman, K. A. Brown, and T. Ranzani, "Magnetorheological fluid-based flow control for soft robots," 2020. DOI: 10.1002/aisy.202000139. [Online]. Available: https://doi.org/10.1002/aisy.202000139..

[37] Y. Miyaki and H. Tsukagoshi, "Self-excited vibration valve that induces traveling waves in pneumatic soft mobile robots," *IEEE Robotics and Automation Letters*, vol. 5, pp. 4133–4139, 3 Jul. 2020, ISSN: 23773766. DOI: 10.1109/LRA.2020.2978455.

[38] M. Raeisinezhad, N. Pagliocca, B. Koohbor, and M. Trkov, "Intellipad: Intelligent soft robotic pad for pressure injury prevention," vol. 2020-July, Institute of Electrical and Electronics Engineers Inc., Jul. 2020, pp. 685–690, ISBN: 9781728167947. DOI: 10.1109/AIM43001.2020.9158916.

[39] M. Salerno, J. Paik, and S. Mintchev, "Oripixel, a multi-dofs origami pixel for modular reconfigurable surfaces," *IEEE Robotics and Automation Letters*, vol. 5, pp. 6988–6995, 4 Oct. 2020, ISSN: 23773766. DOI: 10.1109/LRA.2020.3028054.

[40] S. Schlatter, G. Grasso, S. Rosset, and H. Shea, "Inkjet printing of complex soft machines with densely integrated electrostatic actuators," 2020. DOI: 10.1002/aisy.202000136. [Online]. Available: https://doi.org/10.1002/aisy.202000136..

[41] Y. Sun, M. Li, M. H. Ang, P. Qi, and R. C. H. Yeow, "Fiber pattern optimization for soft robotic pad," *Extreme Mechanics Letters*, vol. 41, Nov. 2020, ISSN: 23524316. DOI: 10.1016/j.eml.2020.101055.

[42] Y. Sun, M. Li, H. Feng, *et al.*, "Soft robotic pad maturing for practical applications," *Soft Robotics*, vol. 7, pp. 30–43, 1 Feb. 2020, ISSN: 21695180. DOI: 10.1089/soro.2018.0128.

[43] J. K. Zou, M. K. Yang, and G. Q. Jin, "A five-way directional soft valve with a case study: A starfish like soft robot," Institute of Electrical and Electronics Engineers Inc., Sep. 2020, pp. 130–134, ISBN: 9781728198880. DOI: 10.1109/CACRE50138.2020.9230177.

[44] D. Drotman, S. Jadhav, D. Sharp, C. Chan, and M. T. Tolley, "Electronics-free pneumatic circuits for controlling soft-legged robots," *Science Robotics*, vol. 6, 51 Feb. 2021, ISSN: 24709476. DOI: 10.1126/SCIROBOTICS.AAY2627.

[45] *Haptic technology for vr and robotics - tactile, force, and motion*, Mar. 2021. [Online]. Available: https://haptx.com/technology/.

[46] S. Hoangid, K. Karydisid, P. Brisk, and W. H. Groverid, "A pneumatic random-access memory for controlling soft robots," 2021. DOI: 10.1371/journal.pone.0254524. [Online]. Available: https://doi.org/10.1371/journal.pone.0254524.

[47] L. Jin, A. E. Forte, and K. Bertoldi, "Mechanical valves for on-board flow control of inflatable robots," 2021. DOI: 10.1002/advs.202101941. [Online]. Available: https://doi.org/10.1002/advs.202101941.

[48] K. Liu, F. Hacker, and C. Daraio, "Robotic surfaces with reversible, spatiotemporal control for shape morphing and object manipulation," *Science Robotics*, vol. 6, 53 2021, ISSN: 24709476. DOI: 10.1126/SCIROBOTICS.ABF5116.

[49] K. McDonald and T. Ranzani, "Hardware methodes for inboard control of fluidcally actuated soft robots," 2021.

[50] e. everydaysight everydaysight, *Brailliant refreshable braille displays*. [Online]. Available: https://www.boundlessat.com/Blindness/Braille-Displays/Brailliant.

[51] M. Sale, *Duckbill valves*. [Online]. Available: http://www.minivalve.com/newsite/?option=com_minivalve&product=12&view=minivalve&lang=en&Itemid=40.

B Digital files

See zip-file